

University of Denver

Digital Commons @ DU

Electronic Theses and Dissertations

Graduate Studies

3-2024

Quantum-Powered Battery Scheduling in Modern Distribution Grids

Diba Ehsani

Follow this and additional works at: <https://digitalcommons.du.edu/etd>



Part of the [Energy Systems Commons](#), and the [Power and Energy Commons](#)



All Rights Reserved.

Quantum-Powered Battery Scheduling in Modern Distribution Grids

Abstract

The rising need for exploiting a novel and evolved computation is an increasing concern in the power distribution system to address the exponential growth of distribution-connected devices. Scheduling numerous battery energy storage systems in an optimal way is one of the emerging challenges that will be more noticeable as the number of batteries, including residential, community, and vehicle batteries, increases in the grid. This thesis focuses on this topic and offers a necessary component in building the quantum-compatible distribution system of the future. Using a constrained quadratic model (CQM) on D-Wave's hybrid solver as well as a binary quadratic model (BQM), this thesis solves the optimal battery scheduling problem for a large number of batteries. To formulate the BQM, a quadratic unconstrained binary optimization (QUBO) format was chosen and in order to fine-tune the QUBO model parameters, a sensitivity analysis was conducted. Numerical simulations, using Tesla Powerwalls, demonstrate promising results of model scalability for a large number of batteries. Additionally, the trend of computational time shows a linear pattern whereas in classical solvers this is exponential.

Document Type

Masters Thesis

Degree Name

M.S.

First Advisor

Amin Khodaei

Second Advisor

Yun-Bo Yi

Third Advisor

Mohammad Matin

Keywords

Power distribution systems, Battery, Energy storage, Binary quadratic model (BQM)

Subject Categories

Electrical and Computer Engineering | Energy Systems | Engineering | Power and Energy

Publication Statement

Copyright is held by the author. User is responsible for all copyright compliance.

Quantum-Powered Battery Scheduling in Modern Distribution Grids

A Thesis

Presented to

the Faculty of the Daniel Felix Ritchie School of Engineering and Computer Science

University of Denver

In Partial Fulfillment

of the Requirements for the Degree

Master of Science

by

Diba Ehsani

March 2024

Advisor: Dr. Amin Khodaei

©Copyright by Diba Ehsani 2024

All Rights Reserved

Author: Diba Ehsani

Title: Quantum-Powered Battery Scheduling in Modern Distribution Grids

Advisor: Dr. Amin Khodaei

Degree Date: March 2024

Abstract

The rising need for exploiting a novel and evolved computation is an increasing concern in the power distribution system to address the exponential growth of distribution-connected devices. Scheduling numerous battery energy storage systems in an optimal way is one of the emerging challenges that will be more noticeable as the number of batteries, including residential, community, and vehicle batteries, increases in the grid. This thesis focuses on this topic and offers a necessary component in building the quantum-compatible distribution system of the future. Using a constrained quadratic model (CQM) on D-Wave's hybrid solver as well as a binary quadratic model (BQM), this thesis solves the optimal battery scheduling problem for a large number of batteries. To formulate the BQM, a quadratic unconstrained binary optimization (QUBO) format was chosen and in order to fine-tune the QUBO model parameters, a sensitivity analysis was conducted. Numerical simulations, using Tesla Powerwalls, demonstrate promising results of model scalability for a large number of batteries. Additionally, the trend of computational time shows a linear pattern whereas in classical solvers this is exponential.

Acknowledgements

I would like to express my sincere gratitude to my advisor, Dr. Amin Khodaei, who inspired me with his bright ideas, generously guided me through the process, and supported me during the challenges of graduate school.

I cannot find a proper word to say how grateful I am for all the support of my partner, Mohammad. I could not have completed this thesis if it were not for the cups of hot tea or the banana and date milkshakes that you have been making for me.

Table of Contents

Chapter 1: Introduction	1
1.1 State of the Art in Battery Scheduling	3
Chapter 2: Battery Scheduling through Constrained Quadratic Modeling.....	7
2.1 Quantum Annealing	7
2.2 Model outline and formulation	8
2.3 Numerical Results	10
2.4 Discussion	14
Chapter 3: Battery Scheduling through Binary Quadratic Modeling	15
3.1 Model Outline and Formulation.....	15
3.1.1 Quadratic Unconstrained Binary Optimization Formulation.....	20
3.2 Numerical Results	21
3.2.1 Finding the initial estimate for β values, the penalty coefficients.....	21
3.2.2 Approach One: A one-factor-at-a-time sensitivity analysis for β	26
3.2.3 Approach two: A systematic approach to sensitivity analysis for β	29
3.2.4 Obtaining the size of the problem.....	29
3.3 Discussion	29
Chapter 4: Conclusion and Future Work	31
References.....	34
Appendix A: Sensitivity analysis, approach one	41
Appendix B: Sensitivity analysis, a systematic approach.....	54

List of Figures

Figure 2- 1: Energy diagram changes over time as the quantum annealing process runs and a bias is applied [32]	8
Figure 2- 2: Battery charging/discharging power and electricity price profile.....	11
Figure 2- 3: The trend of computational time in classical and quantum solvers	12
Figure 3- 1: The results of two simulations with initial values for β of one battery	24
Figure A- 1: The generation of only one battery for initial estimation of β coefficients .	41
Figure A- 2: Total generation of all batteries for initial estimation of β coefficients	41
Figure A- 3: The generation of only one battery for 50% of β_0	42
Figure A- 4: Total generation of all batteries for 50% of β_0	42
Figure A- 5: The generation of only one battery for 150% of β_0	43
Figure A- 6: Total generation of all batteries for 150% of β_0	43
Figure A- 7: The generation of only one battery for 200% of β_0	44
Figure A- 8: Total generation of all batteries for 200% of β_0	44
Figure A- 9: The generation of only one battery for 50% of β_1	45
Figure A- 10: Total generation of all batteries for 50% of β_1	45
Figure A- 11: The generation of only one battery for 150% of β_1	46
Figure A- 12: Total generation of all batteries for 150% of β_1	46
Figure A- 13: The generation of only one battery for 200% of β_1	47
Figure A- 14: Total generation of all batteries for 200% of β_1	47
Figure A- 15: The generation of only one battery for 50% of β_2	48
Figure A- 16: Total generation of all batteries for 50% of β_2	48
Figure A- 17: The generation of only one battery for 150% of β_2	49
Figure A- 18: Total generation of all batteries for 150% of β_2	49
Figure A- 19: The generation of only one battery for 200% of β_2	50
Figure A- 20: Total generation of all batteries for 200% of β_2	50
Figure A- 21: The generation of only one battery for 50% of β_3	51
Figure A- 22: Total generation of all batteries for 50% of β_3	51
Figure A- 23: The generation of only one battery for 150% of β_3	52
Figure A- 24: Total generation of all batteries for 150% of β_3	52
Figure A- 25: The generation of only one battery for 200% of β_3	53
Figure A- 26: Total generation of all batteries for 200% of β_3	53

List of Tables

Table 2- 1: Battery characteristics	11
Table 2- 2: Comparison of classical and quantum solutions for various number of batteries	12
Table 2- 3: Comparison of classical and quantum solutions for various number of batteries considering load balance	13
Table 3- 1: Penalty term value for the inequality constraint (3.2)	18
Table 3- 2: Finding the initial estimates for β coefficients through experiments.....	23
Table 3- 3: The simulation results with initial estimate values for β coefficients (See Figure A- 1, Figure A- 2).....	27
Table 3- 4: Sensitivity analysis based on varying β_0 (See Figure A- 3 to Figure A- 8) ..	27
Table 3- 5: Sensitivity analysis based on varying β_1 (See Figure A- 9 to Figure A- 14)	27
Table 3- 6: Sensitivity analysis based on varying β_2 (See Figure A- 15 to Figure A- 20)	27
Table 3- 7: Sensitivity analysis based on varying β_3 (See Figure A- 21 to Figure A- 26)	28
Table 3- 8: Determining the size of the problem	29

Nomenclature

Indices

i	Index for batteries
t	Index for time
ch	Superscript for battery charging mode
dch	Superscript for battery discharging mode
a	Index for the binary variables x_{ita} to represent an inequality constraint
d	Index for the binary variables y_d to represent an inequality constraint
j, k	Indices for qubits

Sets

\mathcal{T}	The time encompassing the simulation period
\mathcal{B}	Sets of batteries

Parameters

η	Battery roundtrip efficiency
ρ	Electricity price
C_i^{max}	Maximum energy rating of the battery
P_i^{max}	Maximum power rating of battery
D_t	Load demand
β	BQM penalty coefficient
M	The greatest power of 2 that is equal to or smaller than a specified maximum value, i.e., the upper bounds of inequality constraints
h_j	Bias applied to qubit j

J_{jk} Coupling Strength between qubits j and k

$\sigma_{x,z}^{(j)}$ Pauli matrices operating on qubit j

Variables

P_{it}^{ch} Battery charging power

P_{it}^{dch} Battery discharging power

s_{it} Battery operation status in CQM

u_{it} Battery discharging status in BQM

v_{it} Battery charging status in BQM

w_{it} Binary variable used for slack representation

x_{ita} Binary variable used for slack representation

y_d Binary variable used for slack representation

S Slack variable for converting an inequality constraint into an equality constraint

H Hamiltonian

H_I Initial Hamiltonian

H_P Problem Hamiltonian

A, B Annealing Path Functions

Abbreviations

QC quantum computing

QA quantum annealing

CQM constrained quadratic model

BQM binary quadratic model

QUBO quadratic unconstrained binary optimization

QPU quantum processing unit
SDK software development kit
API application programming interface
OFAT one-factor-at-a-time sensitivity analysis
MIP mixed-integer programming

Chapter 1: Introduction

The growing complexity of the grid and the complicated nature of system models are the main reasons that advanced computing solutions will be needed by grid operators in the near future, especially at the distribution level and under the umbrella of smart grids.

Power grid management and optimization, including battery scheduling optimization, is a complex problem, and the computation time of solving this problem grows exponentially with each new variable introduced [1]. As the number of grid energy resources and smart loads continues to grow [2], the complexity and computation time of this optimization will only increase further.

Quantum Computing (QC), which is computation using quantum mechanical phenomena, has already shown its distinctive practicality and promising potential in various fields [3], [4], and [5]. QC utilizes quantum mechanics properties like superposition and entanglement to address conventionally limited computational issues in power grid management and optimization, which can result in efficient computing [6].

One method of QC that could be applicable to battery scheduling optimization is Quantum Annealing (QA). QA is a probabilistic optimization technique that searches for the global optimum of a given objective function, and it is well-suited for problems with a discrete search space [7]. A QA solution is presented here and compared to the classical solution to examine the viability of QC solutions for battery scheduling optimization in terms of computation time.

A structured review using a taxonomic approach [8] states that QC can surpass current conventional computing for certain applications. They call this an emerging “paradigm,” which is beyond an approach, or merely a perspective, or a tool. It is also discussed that the progress in both quantum software and hardware is making its application come to real life. Authors in [5] raise the growth in mathematical complexities and link it to power system challenges, specifically the studies on the grid of the future. In this regard, they present the vital characteristics of QC and multiple potential and prospective problems that require this technology.

Studies in [9] anticipate that considering the computational efficiency and optimization capability of QC owing to “highly efficient algorithms,” the rate of renewable energy modeling will exponentially increase. Further concerning this, [10] puts forth the gap in research between theoretical physics/computer science and real-life applications. They mention that short-term problems, e.g., in renewable energy, should be recognized to illustrate and exploit the QC potential. Along with insight into the basics of QC in smart grids, state of the art, and description of quantum algorithms, [11] provides multiple real-world case studies in this field.

This thesis investigates the application of quantum computing in distribution grid management, and specifically, focuses on optimal coordination and management of battery energy storage systems. There will be growing applications in which a large number of batteries should be scheduled simultaneously. This would include managing multiple distributed consumer-owned home batteries or electric vehicle (EV) batteries by a distribution aggregator, scheduling multiple batteries by a distribution system operator as part of local market clearing and resource commitment, or the resource-constrained

optimization of idle batteries in a battery swapping station. Considering either of these, large-scale battery management will emerge as a necessary component of future distribution grids which will require fast, accurate, and scalable solutions. The contributions of this thesis include: (1) design and formulation of a QA-based optimal battery scheduling for distribution applications in constrained quadratic model (CQM), (2) comparative studies with state-of-the-art classical solutions to identify computational complexity and scalability, (3) scaling up the problem by reformulating the CQM problem into binary quadratic model (BQM), QUBO format, (4) conducting a sensitivity analysis based on the penalty coefficients of the cost function, and (5) determine the current practical limitations in using QC to solve the large-scale battery scheduling problem. The next subsection provides a literature review on battery scheduling. In Chapter two, the concept of quantum annealing is discussed and the problem modeling compatible with CQM is explained. The numerical results and conclusion are provided in sections 2.2 and 2.3, respectively. In the same manner, in Chapter 3 BQM is discussed. A sensitivity analysis is provided in this section, followed by conclusions and future works in Chapter 4.

1.1 State of the Art in Battery Scheduling

Available studies in the literature have investigated the impact of optimal battery scheduling on the efficient operation of the electricity distribution system. For instance, [12] discusses the importance of the battery charging-swapping system for degrading power outage loss and improving the resilience of offshore-island renewable distribution systems. Using a mixed-integer linear programming model, the proposed model provides the optimal solutions based on a 1-hour scheduling step.

Authors in [13] discuss that through intelligent management of distributed resources, such as energy storage, the operation cost of interconnected systems could dramatically drop. By applying particle swarm optimization, they attain the objective of optimal dispatch, which is sensitive to price, and in this way, illustrate the economic effect of selling stored energy at expensive hours. The results in [14] show that appropriate battery scheduling can increase the lifetime of the multi-battery power supply subsystems. The paper comes to this conclusion by using multiple scheduling algorithms.

The impact of battery scheduling on solar power smoothing is addressed through a linear programming formulation in [15]. The authors conclude that this results in reduced net demand due to the intermittent nature of solar PV output, reduction in peak demand, and progress in the voltage profile. Using model predictive control, [16] investigates and simulates demand response by means of battery scheduling along with heating ventilation air conditioning. This is done through co-optimization which results in minimized annual electricity bills simultaneously happening with no discomfort for residents.

In [17], the day-ahead scheduling with distributed energy storage devices is investigated by using mixed-integer linear programming that brings about the impact of their method in terms of an optimization tool. The effects of optimality of battery scheduling, as well as solar PV panels on the electric utility, is discussed in [18] in terms of various problems like unit commitment, peak load shaving, locational marginal pricing, and management of branch congestions.

In [19] and [20] battery's optimal operation is discussed using linear, dynamic programming, and peak shaving control strategies. Along with cost analysis, [21] presents the optimal operation of vanadium redox battery using dynamic programming.

They analyze off-grid and then grid-connected systems. In [22] a comprehensive model for battery scheduling and sizing is proposed, considering impactful factors like the distinctive battery features, and distribution network-microgrid coordination. Their results show that their model can determine the battery technology as well, along with accurate and practical solutions.

More recent studies, e.g., [23] and [24], apply machine learning techniques like deep reinforcement learning and Q-learning for battery scheduling. They thoroughly discuss the impact of the smart charge-discharge scheduling of batteries, which includes preventing irreversible damages due to optimal system's thermal profiles, and battery lifetime; to be more specific, attaining linear gain of system lifetime owing to the nonlinear property of batteries.

The models developed in [25] take load demand uncertainty into account and solve it by analytically considering forecast error and system parameters. They conclude that their method brings about the global minimum solution and lessens the computational complexity of battery scheduling. Other studies, such as the one proposed in [26], aim at minimizing emissions and cost simultaneously. Authors in [26] use a fuzzy satisfying approach and flexible load management and conclude that their method lessens the set of optimal solutions to a meaningful size and is generic, i.e., there would be no need for decision making parameters information.

Using particle swarm optimization, authors of [27] improve the control of charge-discharge of a lithium-ion battery. Their results demonstrate that the robustness of their method for energy storage system scheduling can reduce both energy consumption and the cost of energy usage. Ref. [28] proposes a two-level approach for faster computation:

a dynamic programming approach at certain active hours of the day, and rule-based algorithms at rest of the time. In order to optimally schedule the battery, [29] provides a Coral Reefs optimization algorithm with substrate layers and concludes that it saves up to 10% of costs compared to the conventional method. However, [30] argues that their methodology requires further credibility studies.

These studies provide insights into the importance of battery scheduling and present various methods and perspectives helping this goal; however, the topic of scalability when many batteries are considered is not thoroughly investigated. This is an important piece of the puzzle needed to study for building quantum-compatible distribution systems of the future.

Chapter 2: Battery Scheduling through Constrained Quadratic Modeling

A constrained quadratic model (CQM) is a type of mathematical model that is used in optimization problems. It is characterized by its focus on quadratic objectives and explicitly defined constraints. The variables can be either binary or integer.

2.1 Quantum Annealing

Quantum annealing (QA) is a form of adiabatic quantum computation and probabilistic optimization technique that utilizes quantum physics phenomena, including quantum entanglement, superposition, and tunneling. QA searches for the global optimum of a given objective function, and it is well-suited for problems with a discrete search space [7], such as combinatorial optimization problems with a range of solutions.

The QA algorithm works by taking a Hamiltonian, H , in the form [31]:

$$H = A H_I + B H_P \quad (2.1)$$

where H_I is the initial Hamiltonian, H_P is the problem Hamiltonian, and A and B are annealing path functions. The initial Hamiltonian describes conditions at the start of the annealing process when all qubits are in a superposition state of 0 and 1, while the problem Hamiltonian describes the ground state of the qubits. The initial Hamiltonian and problem Hamiltonian can be written as follows, respectively:

$$H_I = \sum_{(j)} \sigma_x^{(j)} \quad (2.2)$$

$$H_P = \sum_{(j)} h_j \sigma_z^{(j)} + \sum_{jk} J_{jk} \sigma_z^{(j)} \sigma_z^{(k)} \quad (2.3)$$

where $\sigma_{x,z}^{(j)}$ are Pauli matrices operating on qubit q_j , and h_j and J_{jk} represent biases and coupling strengths applied to the qubits in the annealing process. In the beginning of the annealing process, $A = 1$ and $B = 0$, and at the end, $A = 0$ and $B = 1$. This means that the overall Hamiltonian H is evolving from the initial Hamiltonian into the problem Hamiltonian as a magnetic field is passed over the quantum processing unit and the annealing process progresses. At the end of the annealing, the final ground state described by the problem Hamiltonian has a probability of being the optimal solution. In other words, as the QA process begins, the Hamiltonian evolves from its initial state into its ground state, and that ground state has a probability of representing the optimal solution to the given optimization problem. This can be seen in Figure 2- 1, where energy diagrams (a) and (b) represent the initial state of the Hamiltonian, and energy diagram (c) represents the ground state of the Hamiltonian [34].

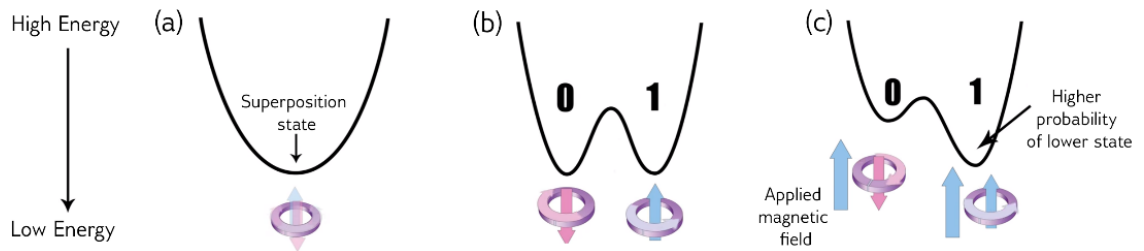


Figure 2- 1: Energy diagram changes over time as the quantum annealing process runs and a bias is applied [32]

2.2 Model outline and formulation

Although the battery scheduling problem is frequently solved through conventional mixed-integer programming (MIP)-based approaches, in this thesis, a quantum-compatible model is developed. The proposed model is QA-based and formulated using a

Constrained Quadratic Model (CQM). The formulation of a problem, whether it be classical computing or quantum, must be compatible with its computing method, the computer associated with it, as well as being understandable for its software. For this thesis, the D-Wave quantum computer [33] is used with hybrid quantum-classical solver. This type of solver minimizes the objective function through a combination of classical heuristics and QA.

The proposed battery scheduling model aims to minimize the total operating cost of a set of batteries (2.4) subject to charging and discharging constraints (2.5)– (2.8).

$$\min \sum_i \sum_t \rho_t (P_{it}^{ch}) \tau \quad (2.4)$$

where ρ is the electricity price at each timestep. The objective is to minimize the total scheduling cost, which includes the cost of purchasing electricity to charge the batteries.

$$C_i^{min} \leq C_{it} \leq C_i^{max} \quad \forall i \in \mathcal{B}, \forall t \in \mathcal{J} \quad (2.5)$$

$$0 \leq P_{it}^{dch} \leq P_i^{max} s_{it} \quad \forall i \in \mathcal{B}, \forall t \in \mathcal{J} \quad (2.6)$$

$$0 \leq P_{it}^{ch} \leq P_i^{max} (1 - s_{it}) \quad \forall i \in \mathcal{B}, \forall t \in \mathcal{J} \quad (2.7)$$

$$C_{it} = C_{i(t-1)} - \frac{P_{it}^{dch} \tau}{\eta_i} + P_{it}^{ch} \tau \quad \forall i \in \mathcal{B}, \forall t \in \mathcal{J} \quad (2.8)$$

$$\sum_i (P_{iT}^{dch}) = D_T \quad T = \text{Peak Hour} \quad (2.9)$$

The battery's stored energy is limited by its minimum and maximum energy ratings (2.5).

The binary variable s shows the battery operational status. When the battery is charging, this status indicator is zero, and when the battery is discharging, this status indicator is one. At an idle state, the binary variable s could be either zero or one. The battery rated

charging and discharging powers are limited by its maximum (nominal) power rating as represented in (2.6) and (2.7). The stored energy at each time period is calculated based on the existing stored energy as well as the charging and discharging powers as shown in (2.8). The roundtrip efficiency of the battery (η) is also considered in this equation. In (2.9) the load balance for each hour is considered in which the load must be equal to the sum of net generation of all batteries. This equation links the independent battery schedules and applies additional limitations to satisfy external grid-imposed requirements.

2.3 Numerical Results

This study uses Ocean as a Software Development Kit (SDK) [34] to interact with the D-Wave quantum computer, here the Hybrid solver for CQM problems, version 1.6. As for the application programming interface (API) for samplers, dimod was imported, which contains classes for quadratic models and their samplers. This study uses D-Wave's Ocean SDK and LeapHybridSolver [35] for all QA simulations. Classical simulations were run using branch-and-cut via CPLEX [36].

In Ocean, the problem is first approached as a quadratic model. After the problem is reformulated as a quantum-compatible problem, optimal solutions are found by sampling. The solver returns a sample set, which consists of not only multiple solutions to the given problem, but also information like computation time and chain breaks. The credibility of the proposed method for battery scheduling is simulated on Tesla Powerwall+ and Tesla Powerwall2. These are integrated lithium-ion battery systems and products of Tesla Energy [37]. The battery characteristics are shown in Table 2- 1. The electricity price is based on [38].

Table 2- 1: Battery characteristics

Name of battery	Technology	Round trip efficiency	Energy capacity	Power rating
Tesla Powerwall+	Lithium-ion	90%	13.5 kWh	7 kW
Tesla Powerwall2	Lithium-ion	90%	13.5 kWh	5 kW

Figure 2- 2 shows an example charging/discharging schedule for one of the simulated batteries. In the optimal solution, the battery is charged during low-price hours and discharged at high-price hours as expected.

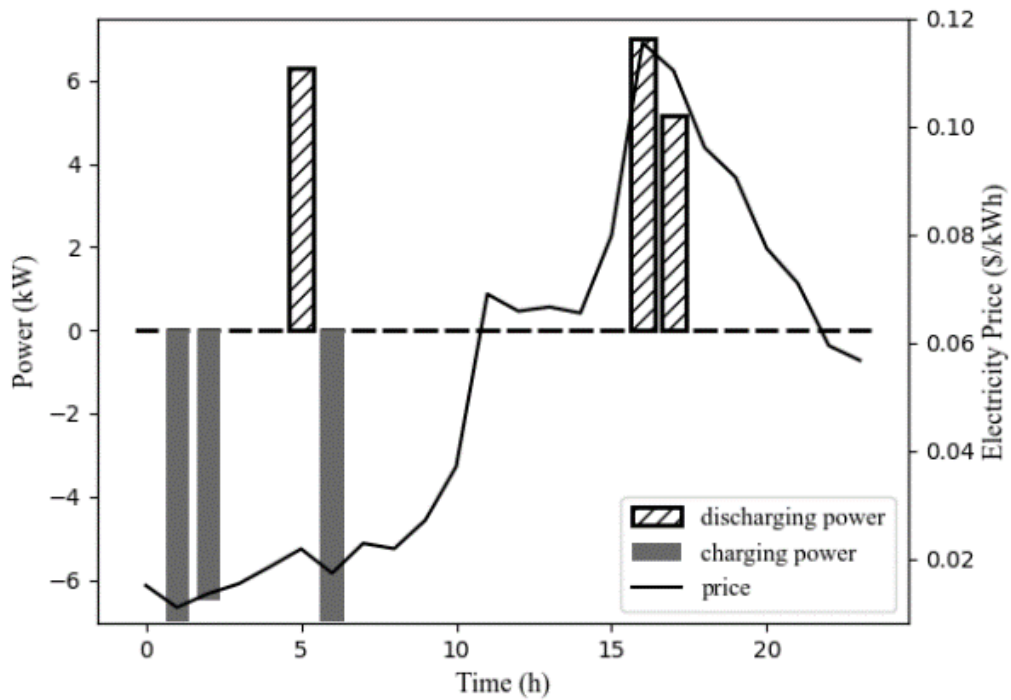


Figure 2- 2: Battery charging/discharging power and electricity price profile

Table 2- 2 shows the simulation results for up to 150 batteries, including the results from a classical solver, CPLEX using branch-and-cut in this case, as well as the proposed quantum model. At first glance, the computation time for the classical solver may look better. However, for larger systems, the “trend” in the computation time must be

considered. As shown in Figure 2- 3, even though the classical approach is fast for small numbers of batteries, the overall trend of the CPLEX solver using branch-and-cut method computation time increases exponentially, whereas, for Hybrid CQM Solver, it is less drastic and presents a more linear trend. This means that by increasing the number of variables and constraints, the computation time will increase linearly.

Table 2- 2: Comparison of classical and quantum solutions for various number of batteries

# of Batteries	CPLEX cost (\$)	CQM cost (\$)	Absolute relative error (%)	# of Variables	# of Constraints
1	-1.20	-1.23	2.38	96	97
2	-2.40	-2.40	0.00	192	194
10	-11.99	-11.59	3.37	960	970
50	-59.96	-58.88	1.79	4800	4850
70	-83.94	-82.65	1.54	6720	6790
100	-119.91	-118.27	1.37	9600	9700
120	-143.90	-142.55	0.94	11520	11640
130	-155.89	-154.71	0.76	12480	12610
140	-167.88	-166.58	0.78	13440	13580
150	-179.87	-19.62	89.09	14400	14550

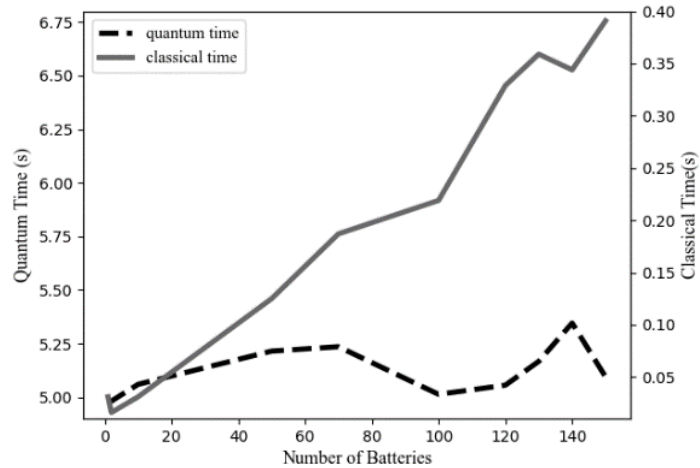


Figure 2- 3: The trend of computational time in classical and quantum solvers

This shows that the quantum model offers better scalability and advocates that for large-scale systems the QC approach is expected to achieve the solution faster than the classical computing approach. The table further shows that the QC results have a small relative error, however this increases significantly for systems with more than 142 batteries. The limitation in the sample data stems from D-Wave’s hardware and software restrictions. There is currently a limited number of binary variables and constraints that could be managed by D-Wave when solving a CQM problem, and the choice of 150 batteries is a result of this number. As the technology matures, we expect to be able to solve a much larger problem using the exact same model developed in this thesis. The small variations in the computation time for various cases are a direct result of the noise inherent in quantum computations, as well as the communications needed between the computation platform and the remote commercial quantum computer.

To further show the performance of the proposed model in solving constrained models, the load balance equation was applied, however only to one hour to represent practical grid operation. The selected hour was hour 18, assuming that the grid operator plans to acquire specific power from the batteries in the system in that hour. The results are shown in Table 2- 3.

Table 2- 3: Comparison of classical and quantum solutions for various number of batteries considering load balance

# of Batteries	CPLEX cost (\$)	CQM cost (\$)	Absolute relative error (%)	# of Variables	# of Constraints
1	-1.17	-1.17	0.00	96	98
2	-2.32	-2.32	0.00	192	195
10	-11.58	-11.41	1.39	960	971
50	-57.88	-56.67	2.08	4800	4851
70	-81.03	-80.30	0.90	6720	6791
100	-115.75	-114.90	0.74	9600	9701

120	-138.90	-137.97	0.67	11520	11641
130	-150.48	-149.40	0.72	12480	12611
140	-162.06	-160.87	0.73	13440	13581
150	-173.63	-19.38	88.84	14400	14551

For each battery, the schedule is adjusted to create a practical and meaningful link between the batteries and the optimized cost, in accordance with the load balance constraint. The results indicate that the proposed model could provide acceptable results in a very limited time even for constrained cases, further proving the acceptable performance of the proposed model. Similar conclusions can be made regarding the computation time and accuracy as in the previous case.

2.4 Discussion

A quantum computing-based model for battery scheduling was proposed in this chapter, using D-Wave's hybrid solver for CQM which is based on a quantum annealing approach. This model was tested on up to 150 batteries of Tesla Powerwall+. The simulation results showed that the running time of this method linearly increases by growth in the number of batteries, whereas this trend becomes exponential in a classical solver. This offers a potential scalability benefit in solving large-scale battery scheduling problems.

Chapter 3: Battery Scheduling through Binary Quadratic Modeling

As stated in the previous chapter, quantum annealing (QA) is a probabilistic optimization technique that falls under the umbrella of adiabatic quantum computing. It uses various quantum phenomena to achieve the objective of finding low-energy solutions for a problem. D-Wave, a quantum computing company, has implemented QA in their quantum computers and quantum processing units (QPUs), and the qubits of the QPU require the problem to be mapped by a binary quadratic model (BQM). Our motivation for using BQM is to increase the size of the problem after applying CQM since the D-Wave's QPU are originally mapped with BQM. In addition, the binary variables are more efficient than CQM's integer variables.

3.1 Model Outline and Formulation

BQM has two forms of formulation: the Ising model and Quadratic Unconstrained Binary Optimization (QUBO). One of the approaches to form an optimization problem in a mathematical structure is by describing it in QUBO format. In QUBO, variables can only take binary values (i.e., 0 and 1.) Also, unlike conventional optimization problems which involve explicit constraints that define the feasibility of the problem, in QUBO, constraints are added to the objective function as penalty terms. In this way, minimizing the objective function that is designed in a manner that penalizes undesired configurations will naturally lead to feasible and optimal solutions.

To formulate the problem in QUBO-appropriate format, first, the problem needs to be defined, meaning the objective function that should be minimized and constraints that explain the feasible region of the solutions are identified. Second, the problem needs to have a mathematical expression with correct variables. Then, the equality and inequality constraints should form penalty terms, which will be added to the objective function to form one cost equation that needs to be minimized. For example, an equality constraint can be transformed into a term that will be minimized. The approach is moving all the equation elements to one side which will lead to an equality to zero, where minimizing the square of the non-zero side will result in the main equality constraint being enforced. After that, the problem variables should be converted to binary ones. Finally, the objective function and all the penalty terms should be summed up. The CQM-compatible form of the problem that was stated in CQM formulation in the previous chapter, can be reformulated as follows:

$$\min \sum_t \sum_i \rho_t P_{it}^{ch} \quad (3.1)$$

$$u_{it} + v_{it} \leq 1 \quad \forall i \in \mathcal{B}, \forall t \in \mathcal{J} \quad (3.2)$$

$$0 \leq \sum_{t'=0}^t (P_{it'}^{ch} - P_{it'}^{dch}) \leq \eta C_i^{max} \quad \forall i \in \mathcal{B}, \forall t \in \mathcal{J} \quad (3.3)$$

$$\sum_i P_{iT}^{dch} \geq D_T \quad T = \text{Peak hour} \quad (3.4)$$

$$P_{it}^{dch} = P_i^{max} u_{it} \quad \forall i \in \mathcal{B}, \forall t \in \mathcal{J} \quad (3.5)$$

$$P_{it}^{ch} = P_i^{max} v_{it} \quad \forall i \in \mathcal{B}, \forall t \in \mathcal{J} \quad (3.6)$$

As shown in (3.1), the objective is to minimize the total scheduling cost, which includes the cost of purchasing electricity to charge the batteries. In constraint (3.2), u and v , which represent the discharging and charging status of batteries, respectively, cannot be 1 simultaneously. Constraint (3.3) is another expression of constraint (2.8), which ensures that the total energy of batteries at each timestep, which consists of charging power subtracted by discharging power, is within the bounds. It must be summed up over time to ensure its satisfaction during the whole timespan. Constraint (3.4) enforces meeting the demand at peak hours. Basically, the discharging power of all the batteries at peak hour should be larger than the demand. Even though the load balance constraint is an equality one due to the inherent of the power system, it is intentionally chosen to be an inequality constraint to prevent it from getting too much penalized and added to the objective. Equations (3.5) and (3.6) are defined to simplify the problem, i.e., the battery charging/discharging power is assumed to be either 0 or at its maximum value.

As stated earlier, in QUBO, the whole optimization problem should form one single equation. To change the linear inequality constraint (3.2) to an equality constraint, the slack binary variable w is introduced:

$$u_{it} + v_{it} + w_{it} = 1 \quad \forall i \in \mathcal{B}, \forall t \in \mathcal{J} \quad (3.7)$$

Then, the penalty term to represent this inequality constraint will be formed as equation (3.8). By minimizing this penalty term, the constraint (3.2) will be enforced, meaning u and v will have all the feasible values.

$$P(u_{it}, v_{it}, w_{it}) = (u_{it} + v_{it} + w_{it} - 1)^2$$

$$\begin{aligned}
&= 2u_{it}v_{it} + 2v_{it}w_{it} + 2w_{it}u_{it} - u_{it} - v_{it} - w_{it} + 1 \\
&= -u_{it} - v_{it} - w_{it} + 1
\end{aligned} \tag{3.8}$$

In equation (3.8) it was considered that in QUBO, the square of a binary variable is identical to the binary variable since the square of 0 and 1 will make no changes. In other words, $u^2 = u$. Table 3- 1 represents the penalty values for the inequality constraint (3.2) which later transformed into equation (3.7). This table shows how adding a slack variable and forming a penalty term would cause the desired combination of u and v to be chosen, when battery cannot be charged and discharged at the same time, i.e., u and v are not both equal to 1. The minimum of the last column is 0; Consequently, only the $u_{it}, v_{it} = 1$ scenario will not be chosen, as expected. The other feasible combinations of u and v cause minimum penalty value. When $u, v,$ and w equal to 1, $P(u, v, w)$ becomes 4 and will not be chosen.

Table 3- 1: Penalty term value for the inequality constraint (3.2)

u_{it}, v_{it}	$P_{w_{it}=0}$	$P_{w_{it}=1}$	$min P$
0,0	1	0	0
0,1	0	1	0
1,0	0	1	0
1,1	1	4	1

To change the linear inequality of constraint (3.3) to equality constraints, two slack variables are introduced for each side, which are non-negative variables that help transform the inequality into an equality. A slack variable is introduced for each inequality constraint. Equation (3.9) considers $S11$, a slack variable to form the left-hand

side of inequality constraint (3.3). Likewise, $S12$ is presented in equation (3.10) to reformat the right-hand side of inequality constraint (3.3).

$$-\sum_{t'=0}^t (P_{it'}^{ch} - P_{it'}^{dch}) + S11_{it} = 0 \quad (3.9)$$

$$\sum_{t'=0}^t (P_{it'}^{ch} - P_{it'}^{dch}) + \eta C_i^{max} + S12_{it} = 0 \quad (3.10)$$

$S11$ and $S12$ in equations (3.9) and (3.10) can be written as one single slack variable, $S1$. Thus, the two-sided inequality constraint (3.3) becomes:

$$\sum_{t'=0}^t (P_{it'}^{ch} - P_{it'}^{dch}) = S1_{it} \quad (3.11)$$

Where:

$$0 \leq S1_{it} \leq \eta C_i^{max} \quad (3.12)$$

Finally, we convert this modified objective function into a BQM representation, which can be used for QA. In a QUBO-compatible format, we express it as a combination of binary variables (discretizing). For example, we can use binary variables x_{ita} based on powers of 2. In this way, the desired space would be represented by a fewer number of variables. This is crucial regarding the computation time.

$$S1_{it} = 2^0 x_{it0} + 2^1 x_{it1} + 2^2 x_{it2} + \dots + 2^M x_{itM} \quad (3.13)$$

Where M is the largest power of 2 that is less than or equal to the given maximum value, ηC_i^{max} .

$$\sum_{t'=0}^t (P_{it'}^{ch} - P_{it'}^{dch}) = 2^0 x_{it0} + 2^1 x_{it1} + 2^2 x_{it2} + \dots + 2^M x_{itM} \quad (3.14)$$

The process of reformulating the problem into a QUBO-compatible format will be the same process for the inequality constraint (3.4):

$$\sum_i P_{iT}^{dch} = 2^0 y_0 + 2^1 y_1 + 2^2 y_2 + \dots + 2^{M'} y_{M'} \quad (3.15)$$

Where M' is the largest power of 2 that is less than or equal to the given maximum value, D_T .

3.1.1 Quadratic Unconstrained Binary Optimization Formulation

The objective function and the prepared penalty terms should be combined to form one equation to be minimized, as shown in equation (3.16).

$$\begin{aligned} C(u, v, w, x, y) = & \sum_i \sum_t \rho_t P_i^{max} v_{it} + \\ & \beta_1 * \sum_i \sum_t (u_{it} + v_{it} + w_{it} - 1)^2 + \\ & \beta_2 * \sum_i \sum_t \left(\left(\sum_{t'=0}^t (P_i^{max} v_{it'} - P_i^{max} u_{it'}) \right) \right. \\ & \quad \left. - (2^0 x_{it0} + 2^1 x_{it1} + 2^2 x_{it2} + \dots + 2^M x_{itM}) \right)^2 + \\ & \beta_3 * \left(\sum_i P_i^{max} u_{iT} \right. \\ & \quad \left. - (2^0 y_0 + 2^1 y_1 + 2^2 y_2 + \dots + 2^{M'} y_{M'}) \right)^2 \end{aligned} \quad (3.16)$$

Where the first term specifies the objective function, and the rest are penalty terms associated with constraints (3.2), (3.3), and (3.4), respectively. The penalty terms need to

be weighted by penalty coefficients, β values, to adjust their importance. Otherwise, they could overpower the objective.

3.2 Numerical Results

This study uses Ocean's Software Development Kit (SDK) to interact with D-Wave quantum computers, specifically, the Hybrid solver for BQM problems (i.e., `hybrid_binary_quadratic_model_version2`). For the sampler's API, `dimod` was imported, which contains classes for quadratic models and their samplers. This study uses D-Wave's Ocean SDK and `LeapHybridSolver` for all QA simulations.

In Ocean, the problem is first approached as a quantum-compatible model, i.e., a binary quadratic model. After that, optimal solutions are found by sampling. The solver returns a sample set, which consists of not only multiple solutions to the given problem, but also information like computation time. In this research, the credibility of the proposed method for battery scheduling is verified on Tesla Powerwall+ and Tesla Powerwall2. Both Powerwall+ and Powerwall2 are integrated lithium-ion battery systems which are products of Tesla Energy [34]. The battery characteristics are shown in Table 2-1 in chapter 2. The electricity price is based on the price profile provided in [38].

3.2.1 Finding the initial estimate for β values, the penalty coefficients

The objective function of this problem in QUBO format has terms that consist of binary variables, and the coefficients, β_1 , β_2 , and β_3 , are weights for penalties that need to be optimized. There are various approaches to finding the optimal values for these β coefficients, including but not limited to grid search, gradient descent, heuristics or metaheuristics, specialized solvers, and experimentation through simulation. In this

research, experimentation through simulation method was applied to find proper penalty coefficients through an iterative approach.

To have sensible initial guesses for β coefficients, the characteristics of the problem and each penalty were considered. β_1 enforces the constraints that each battery cannot be charged and discharged simultaneously. Since this scenario is physically impossible, it should be the highest penalty to strictly enforce this rule. An initial guess was based on the highest cost in the objective function with a relatively high penalty factor (first row in Table 3- 2.) For β_2 a moderate value was expected to keep P^{ch} and P^{dch} within bounds, e.g., the estimated cost of operating outside the desired range. To ensure meeting the demand, a smaller value than β_1 was chosen for β_3 , e.g., five times the cost of not meeting the demand.

In this trial-and-error approach, to adjust the β values systematically, it was attempted to adjust β coefficients based on the constraint importance. By calculating the values of each penalty and the objective function value, the costs for each simulation the β coefficient values were set proportionally. In other words, each cost was normalized (see β_2 value in row 3 of Table 3- 2).

Nevertheless, the impact of the number of batteries should also be considered. As shown in equation (3.16), the relationship between the number of batteries and β values in the cost function is not always linear. By an increase in the number of batteries, the overall capacity of the of the system also increases. This may mean that the β value for each penalty needs to be re-evaluated to make sure they scale appropriately with the increased system capacity. Also, the relative importance of penalties might change with changes in the size of the problem.

A detailed log of a set of simulations is provided in Table 3- 2. In addition to β coefficients present in equation (3.16), β_0 was added for the objective function. The penalty values show the order of the magnitude of penalties. Energy represents the total cost based on equation (3.16).

Table 3- 2: Finding the initial estimates for β coefficients through experiments

# of Batt	Time span (h)	Run time (s)	Energy	Obj. val.	Penalty1	Penalty2	Penalty3	β_0	β_1	β_2	β_3
10	8	3.79	45012923	3.18	10^7	10^7	-	1	8960975.99 (500 * highest cost in the objective function)	1	1
10	8	3.79	5701770	4.32	10	10^6	-	1	1	1	1
10	8	3.79	41	3.784	10	10	-	1	1	$1/10^6 \approx 1.75e-06$	1
10	8	3.79	70	2.56	0	10	10	1	100	1.75E-06	10

Following the approach described earlier, some initial estimates are determined for β values. Figure 3- 1 and Figure 3- 2 present the results of two simulations. Figure 3- 1 represents examples of charging or discharging schedules for one of the simulated batteries which is chosen randomly. In the optimal solution, the battery is charged during low-price hours and discharged at high-price hours as expected according to the objective function. The constraint that limits the battery to be charged and discharged simultaneously is met. Figure 3-2 shows the total generation of all batteries for each

simulation. At the peak hour which is $t=7$, the total discharge of all batteries is equal to demand at that time, as expected according to the last constraint, the load balance.

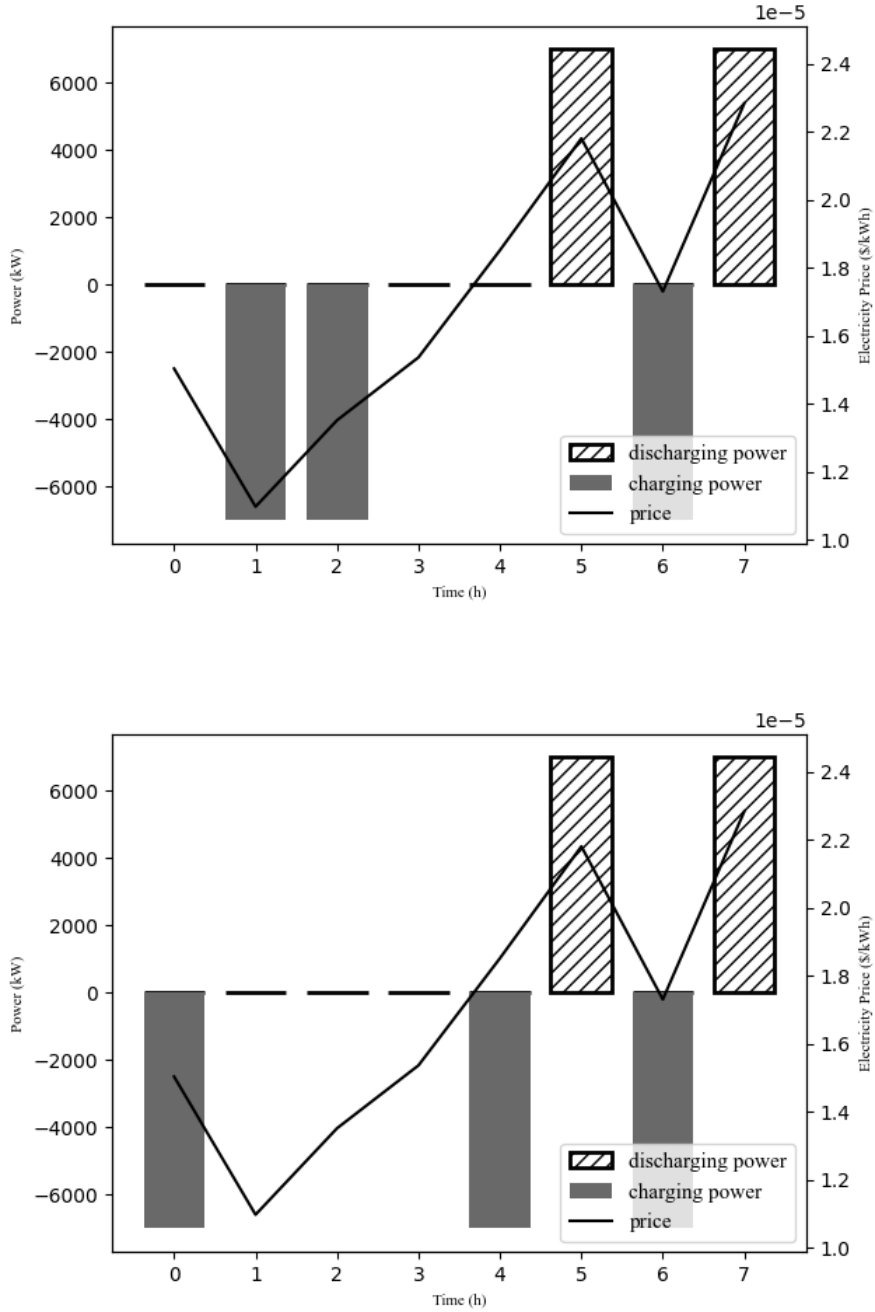


Figure 3- 1: The results of two simulations with initial values for β of one battery

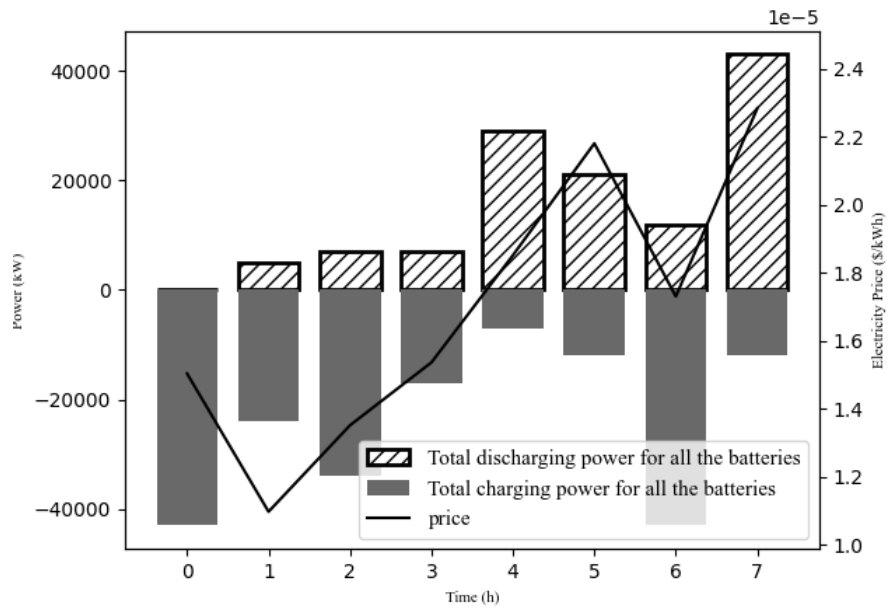
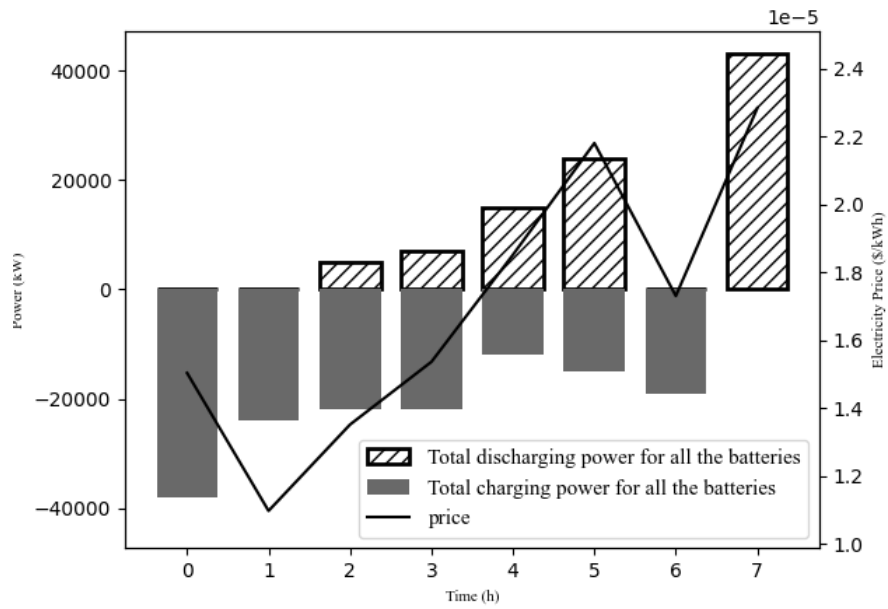


Figure 3- 2: The results of two simulations with initial estimates values for β for the total generation of all batteries

3.2.2 Approach One: A one-factor-at-a-time sensitivity analysis for β

Having initial estimates for β values is the starting point for conducting a sensitivity analysis for the battery scheduling problem. This sensitivity analysis involves systematically varying the β coefficients within a certain range and observing how these variations affect the solution. The goal is to understand the robustness of the solutions to changes in these coefficients and to identify the optimal range for each β .

The proposed range for each β must be realistic and based on the initial estimates. In this case, 50% below and 200% above those initial estimates represent logical starting points. Then, each range was discretized by a sensible granularity. Although more granular intervals provide more detailed information, due to the limitation in quantum computational time and available solver access, the intervals cannot be very small discrete chunks.

Then, by systematically changing one β while keeping the rest at baseline values, the simulation was run iteratively. This process was repeated for each β . The approach of changing one parameter at a time is called one-factor-at-a-time (OFAT) sensitivity analysis.

Table 3- 3 to Table 3- 7 provide simulation results and summarize this process. The first figures in each row of the tables show examples of charging/ discharging schedules for one of the simulated batteries which is chosen randomly. In the optimal solution, the battery is charged during low-price hours and discharged at high-price hours as expected. The second figure in each row of the tables demonstrates the total generation of all batteries. These figures are provided in Appendix A. The penalty values show the order of the magnitude of penalties.

Table 3- 3: The simulation results with initial estimate values for β coefficients (See Figure A- 1, Figure A- 2)

# of Batteries	Time span (h)	Run time (s)	Energy	Obj. val.	Penalty1 val.	Penalty2 val.	Penalty3 val.	β_0	β_1	β_2 ($\times 10^{-6}$)	β_3
10	8	3.79	63.44	2.35	0	10	10	1	100	1.75	10

Table 3- 4: Sensitivity analysis based on varying β_0 (See Figure A- 3 to Figure A- 8)

# of Batteries	Time span (h)	Run time (s)	Energy	Obj. val.	Penalty1 val.	Penalty2 val.	Penalty3 val.	β_0	β_1	β_2 ($\times 10^{-6}$)	β_3
10	8	3.80	580.26	1.67	10^2	10^2	10	0.5	100	3.5	10
10	8	3.80	183.85	4.12	0	10^2	0	1.5	100	3.5	10
10	8	3.80	919.60	7.33	10^2	10^2	0	2	100	3.5	10

Table 3- 5: Sensitivity analysis based on varying β_1 (See Figure A- 9 to Figure A- 14)

# of Batteries	Time span (h)	Run time (s)	Energy	Obj. val.	Penalty1 val.	Penalty2 val.	Penalty3 val.	β_0	β_1	β_2 ($\times 10^{-6}$)	β_3
10	8	3.80	276.60	2.98	10^2	10	10	1	50	1.75	10
10	8	3.80	148.27	2.96	0	10^2	10	1	150	1.75	10
10	8	3.80	96.22	2.35	0	10	10	1	200	1.75	10

Table 3- 6: Sensitivity analysis based on varying β_2 (See Figure A- 15 to Figure A- 20)

# of Batteries	Time span (h)	Run time (s)	Energy	Obj. val.	Penalty1 val.	Penalty2 val.	Penalty3 val.	β_0	β_1	β_2 ($\times 10^{-6}$)	β_3
10	8	3.79	103.94	2.64	0	10	10	1	100	.875	10
10	8	3.80	294.72	2.86	10^2	10	0	1	100	2.63	10
10	8	3.80	165.34	2.90	0	10^2	0	1	100	3.5	10

Table 3- 7: Sensitivity analysis based on varying β_3 (See Figure A- 21 to Figure A- 26)

# of Batteries	Time span (h)	Run time (s)	Energy	Obj. val.	Penalty1 val.	Penalty2 val.	Penalty3 val.	β_0	β_1	β_2 ($\times 10^{-6}$)	β_3
10	8	3.80	205.15	3.49	10^2	10^2	0	1	100	3.5	5
10	8	3.80	730.29	3.17	10^2	10^2	10	1	100	3.5	15
10	8	3.79	411.44	2.88	10^2	10	10	1	100	3.5	20

For analyzing the results of the simulations, the simulation outcomes which are objective function values, penalty terms values, and the total energy (cost) must be evaluated. Then, to understand the trends and patterns by changing each β , their effect on outcomes needs to be monitored.

For example, for changes in β_0 , β_1 , and β_3 it was observed that the initial estimate values make more sense in terms of the total energy, objective function cost, and the decrease in the penalties. In the same manner, lower values of β_2 make the system too rigid; meaning the system is not very adaptable to changes in inputs. Additionally, those changes made the system less capable of balancing multiple terms and made the performance of the system inflexible.

However, increasing β_2 to a certain point, 200% of the initial estimate, significantly improves the constraints satisfaction. The 200% was the threshold where at that certain point changes in β_2 had a significant impact on the results. In every iteration the results were compared against the baseline, i.e., initial estimates. If the results were improved in terms of lower penalty values, the updated β values were implemented moving forward. Therefore, there was a feedback loop to improve the β values during the iterative simulations.

3.2.3 Approach two: A systematic approach to sensitivity analysis for β

Based on the order of magnitude of obtained penalty terms, the beta values would make better sense when starting at small values like 1e-2. Sensitivity analysis on beta values was performed with three options for each beta: 1e-2, 1, 100. Given three penalty terms when each has one specific penalty coefficient (beta), the number of possible cases is equal to $3 \times 3 \times 3 = 27$. Where each term represents the three possible values for each of those three betas. The results of this study are presented in Appendix B.

3.2.4 Obtaining the size of the problem

After the optimal penalty coefficients were analyzed, the size of the problem was determined. Table 3- 8 demonstrates the results of simulations for various number of batteries.

Table 3- 8: Determining the size of the problem

# of Batteries	Time span (h)	Run time (s)	Energy	Obj. val.	Penalty1 val.	Penalty2 val.	Penalty3 val.	β_0	β_1	β_2 ($\times 10^{-6}$)	β_3
100	8	68.9	15434	38.7	10^4	10^3	10	1	100	3.5	10
500	8	417.2	126781	198.4	10^6	10^{-2}	10^5	1	100	3.5	10
1000	8	599.6	171437	395.2	10^5	10^4	10^3	1	100	3.5	10
2000	8	597.0	2504580	791.0	10^5	10^4	10^6	1	100	3.5	10

3.3 Discussion

To improve the accuracy of results when solving an optimization problem using D-Wave's hybrid solvers, specifically for a BQM, it is necessary to fine-tune the model, parameters, coefficients, etc.

By reformulating the constrained optimization problem with continues variables to an unconstrained problem in which all the variables are binary and their relationship is linear

and/or quadratic, along with conducting an OFAT sensitivity analysis based on the penalty coefficients, accurate results were obtained in terms of the objective function and penalty terms values, minimizing the objective, and providing feasible solutions where all the constraints are met.

The sensitivity analysis was performed iteratively, and the pattern was observed in each simulation to see the trends of the outcomes by changes in β values. A feedback loop was applied to update each β coefficient when the results were more satisfactory.

Most importantly, the size of the problem is considerably increased from 142 batteries in the CQM method to around 2000 batteries in the BQM. There is also a significant increase in the number of variables from the BQM method to CQM. For instance, in an 8-hour timespan, the number of variables increases from 3200 binary and integer variables for CQM to 13616 binary variables for the BQM. Additionally, the run time decreases (e.g., around 25% for the same number of batteries and timespan) and the conclusion that was drawn in the previous chapter regarding the linear trend of computational time by a hybrid solver is still valid.

Chapter 4: Conclusion and Future Work

Two quantum computing-based models, using CQM and BQM, for battery scheduling were proposed in this thesis. D-Wave's hybrid solvers, which are based on a quantum annealing approach, were utilized as the solvers.

The CQM model was tested on up to 150 batteries of Tesla Powerwall batteries. The simulation results showed that the running time of the CQM method linearly increases by growth in the number of batteries, whereas this trend becomes exponential in a classical solver such as CPLEX. This offers a potential scalability benefit in solving large-scale battery scheduling problems. The ceiling on the number of batteries was limited by the current limitation, i.e., the number of qubits, associated with quantum computers hardware. However, adding only one qubit to available quantum computers would result in significant improvement in the number of batteries that could potentially be optimized by the CQM solver. Authors of the book [39] explain why by adding only one qubit the size of the problem doubles, which is a promising fact that will cause extraordinary development in the near future.

To overcome the challenges associated with the number of qubits on the size of the problem, a novel BQM model was proposed. This model benefits from binary-only variables that decrease the run time considerably. This QUBO-appropriate model consists of the objective function and all the inequality and equality constraints in the form of penalty terms, all in one single equation.

Each penalty term requires a penalty coefficient, β , which can be adjusted to prevent the constraints overpowering the objective. However, tuning the β values was a challenge. In this case, the initial estimations were obtained through experiments as well as assigning some initial values when the nature of the problem was considered.

To find the optimal range of each β , an OFAT sensitivity analysis based on the penalty coefficients was performed which resulted in accurate results in terms of the objective function and penalty terms values, minimizing the objective, and providing feasible solutions where all the constraints are met.

Considering all the challenges discovered while conducting this research, the following provide some suggestions for future work and continued investigation in this area:

- Applying other quantum solvers: This research implemented hybrid quantum-classical solvers (i.e., BQM and CQM solvers). However, quantum-only solvers such as QBSolv and Advantage Solvers could potentially provide additional insights to improving the scalability.
- Integrating binary and continuous decomposition in the problem structure to speed up the computation time and increase the accuracy of the results. Currently, the CQM method uses an integer-based approach which results in higher accuracy in the expense of computational runtime. The BQM method uses a binary-based approach which improves the computational runtime and its scale considerably in the expense of lower accuracy. Therefore, integrated decomposition is expected to improve computational runtime, scalability, and accuracy.

- Considering other power distribution elements. Currently, this research considers battery as a stationary power asset that needs to be quantum compatible. However, including other power elements such as dynamic power assets (like electric vehicles) and the complexities around those, such as the time constraint on battery to charge/discharge in the case of EVs, could provide additional actionable insights.

References

- [1] Electric Power Research Institute, "Quantum Science & Technology: 2022 Technology Update Across the Energy Industry," 2022.
- [2] Abujarad, Saleh Y., M.W. Mustafa, and J.J. Jamian, "Recent Approaches of Unit Commitment in the Presence of Intermittent Renewable Energy Resources: A Review," *Renewable & sustainable energy reviews*, vol. 70, p. 215–223, 2017.
- [3] S. Koretsky et al, "Adapting Quantum Approximation Optimization Algorithm (QAOA) for Unit Commitmen," in *2021 IEEE International Conference on Quantum Computing and Engineering (QCE)*, 2021.
- [4] Rozhin Eskandarpour, Kumar Ghosh, Amin Khodaei, Aleksii Paaso, "Experimental Quantum Computing to Solve Network DC Power Flow Problem," in *Unpublished*, 2021.
- [5] R. Eskandarpour, K. J. Bahadur Ghosh, A. Khodaei, A. Paaso and L. Zhang, "Quantum-Enhanced Grid of the Future: A Primer," *IEEE Access*, vol. 8, pp. 188993-189002, 2020.
- [6] Y. Zhou et al., "Quantum computing in power systems," *iEnergy*, vol. 1, no. 2, pp. 170-187, 2022.

- [7] S. E. Venegas-Andraca, W. Cruz-Santos, C. McGeoch and M. Lanzagorta, "A cross-disciplinary introduction to quantum annealing-based algorithms," *Contemporary Physics*, vol. 59, no. 2, pp. 174-197, 2018.
- [8] S. S. Gill, et al, "Quantum computing: A taxonomy, systematic review and future directions," *Software: Practice and Experience*, vol. 52, no. 1, pp. 66-114, 2022.
- [9] O. O. Olatunji, P. A. Adedeji, N. Madushele, "Chapter 22 - Quantum computing in renewable energy exploration: status, opportunities, and challenges," in *Design, Analysis, and Applications of Renewable Energy Systems*, Academic Press, 2021, pp. 549-572.
- [10] A. Giani and Z. Eldredge, "Quantum Computing Opportunities in Renewable Energy," *SN Computer Science*, vol. 2, no. 5, p. 393, 2021.
- [11] M. H. Ullah, R. Eskandarpour, H. Zheng and A. Khodaei, "Quantum computing for smart grid applications," *IET Generation, Transmission & Distribution*, vol. 16, no. 21, pp. 4239-4257, 2022.
- [12] Q. Sui, et al, "Optimal scheduling of battery charging–swapping systems for distribution network resilience enhancement," *Energy Reports*, vol. 8, pp. 6161-6170, 2022.
- [13] E. Sortomme and M. A. El-Sharkawi, "Optimal Power Flow for a System of Microgrids with Controllable Loads and Battery Storage," in *2009 IEEE/PES*

Power Systems Conference and Exposition, Optimal Power Flow for a System of Microgrids with Controllable Loads and Battery Storage.

- [14] L. Benini et al., "Extending lifetime of portable systems by battery scheduling," in *Proceedings Design, Automation and Test in Europe. Conference and Exhibition 2001*, 2001.
- [15] R. Karandeh, W. Prendergast and V. Cecchi, "Optimal Scheduling of Battery Energy Storage Systems for Solar Power Smoothing," in *2019 SoutheastCon*, 2019.
- [16] D. T. Vedullapalli, R. Hadidi and B. Schroeder, "Combined HVAC and Battery Scheduling for Demand Response in a Building," *IEEE Transactions on Industry Applications*, vol. 55, no. 6, pp. 7008-7014, 2019.
- [17] G. Haddadian, N. Khalili, M. Khodayar and M. Shahidehpour, "Optimal scheduling of distributed battery storage for enhancing the security and the economics of electric power systems with emission constraints," *Electric Power Systems Research*, vol. 124, pp. 152-159, 2015.
- [18] Bo Lu and M. Shahidehpour, "Short-term scheduling of battery in a grid-connected PV/battery system," *IEEE Transactions on Power Systems*, vol. 20, no. 2, pp. 1053-1061, 2005.
- [19] G. Carpinelli, F. Mottola and L. Perrotta, "Energy management of storage systems for industrial applications under real time pricing," in *2013*

- International Conference on Renewable Energy Research and Applications (ICRERA)*, 2013.
- [20] M. Dabbagh, A. Rayes, B. Hamdaoui and M. Guizani, "Peak shaving through optimal energy storage control for data centers," in *2016 IEEE International Conference on Communications (ICC)*, 2016.
- [21] T. A. Nguyen, M. L. Crow and A. C. Elmore, "Optimal Sizing of a Vanadium Redox Battery System for Microgrid Systems," *IEEE Transactions on Sustainable Energy*, vol. 6, no. 3, pp. 729-737, 2015.
- [22] I. Alsaidan, A. Khodaei and W. Gao, "A Comprehensive Battery Energy Storage Optimal Sizing Model for Microgrid Applications," *IEEE Transactions on Power Systems*, vol. 33, no. 4, pp. 3968-3980, 2018.
- [23] Y. Sui and S. Song, "A Multi-Agent Reinforcement Learning Framework for Lithium-ion Battery Scheduling Problems," *Energies*, vol. 13, no. 8, p. 1982, 2020.
- [24] I. A. T P, R. Roy, S. Siyad, S. Santhosh and V. Rajeev, "Investigation of Choice of State Space for Reinforcement Learning Based Battery Scheduling in Microgrid," in *2022 IEEE International Conference on Signal Processing, Informatics, Communication and Energy Systems (SPICES)*, 2022.
- [25] M.J. Sanjari and H. Karami, "Optimal control strategy of battery-integrated energy system considering load demand uncertainty," *Energy*, vol. 210, p. 118525, 2020.

- [26] H. Pashaei-Didani, S. Nojavan, R. Nourollahi and K. Zare, "Optimal economic-emission performance of fuel cell/CHP/storage based microgrid," *International Journal of Hydrogen Energy*, vol. 44, no. 13, pp. 6896-6908, 2019.
- [27] M. Faisal et al., "Particle swarm optimised fuzzy controller for charging–discharging and scheduling of battery energy storage system in MG applications," *Energy Reports*, vol. 6, pp. 215-228, 2020.
- [28] R. Chedid, A. Sawwas and D. Fares, "Optimal design of a university campus micro-grid operating under unreliable grid considering PV and battery storage," *Energy*, vol. 200, p. 117510, 2020.
- [29] S. Salcedo-Sanz, C. Camacho-Gómez, R. Mallol-Poyato, S. Jiménez-Fernández, J. Del Ser, "A novel Coral Reefs Optimization algorithm with substrate layers for optimal battery scheduling optimization in micro-grids," *Soft Computing*, vol. 20, no. 11, pp. 4287-4300, 2016.
- [30] M. S. H. Lipu et al., "A review of controllers and optimizations based scheduling operation for battery energy storage system towards decarbonization in microgrid: Challenges and future directions," *Journal of Cleaner Production*, vol. 360, p. 132188, 2022.
- [31] H. N. Djidjev, G. Chapuis, G. Hahn, and G. Rizk, "Efficient combinatorial optimization using quantum annealing," *unpublished at arXiv preprint, arXiv:1801.08653*, 2018.

- [32] "What is Quantum Annealing?: How Quantum Annealing Works in D-Wave QPUs," D-Wave, [Online]. Available: https://docs.dwavesys.com/docs/latest/c_gs_2.html. [Accessed 12 November 2022].
- [33] D-Wave, [Online]. Available: <https://docs.dwavesys.com/>. [Accessed 13 November 2022].
- [34] D-Wave, "Ocean," D-Wave, [Online]. Available: <https://www.dwavesys.com/solutions-and-products/ocean/>. [Accessed November 2023].
- [35] D-Wave, "Using Leap's Hybrid Solvers," D-Wave, [Online]. Available: https://docs.dwavesys.com/docs/latest/doc_leap_hybrid.html. [Accessed November 2023].
- [36] "Branch and cut in CPLEX," IBM, [Online]. Available: <https://www.ibm.com/docs/en/icos/12.10.0?topic=concepts-branch-cut-in-cplex>. [Accessed November 2023].
- [37] Tesla, [Online]. Available: <https://www.tesla.com/powerwall>.
- [38] A. Khodaei, "Microgrid Optimal Scheduling With Multi-Period Islanding Constraints," *IEEE Transactions on Power Systems*, vol. 29, no. 3, pp. 1383-1392, 2014.

- [39] Grumbling, Emily, and Mark Horowitz, eds., Quantum Computing : Progress and Prospects, Washington, District of Columbia : The National Academies Press, 2019.

Appendix A: Sensitivity analysis, approach one

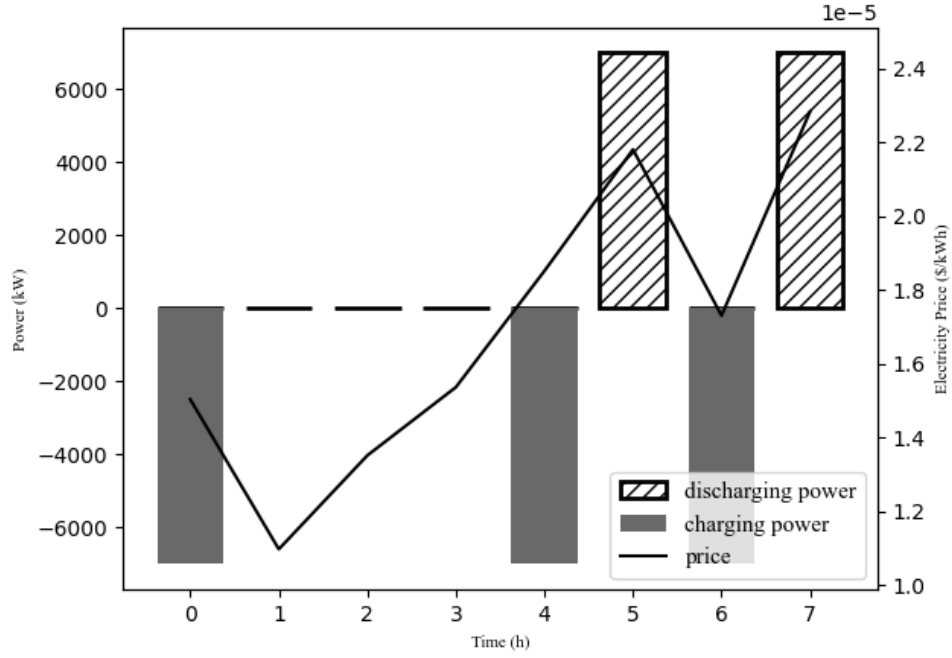


Figure A- 1: The generation of only one battery for initial estimation of β coefficients

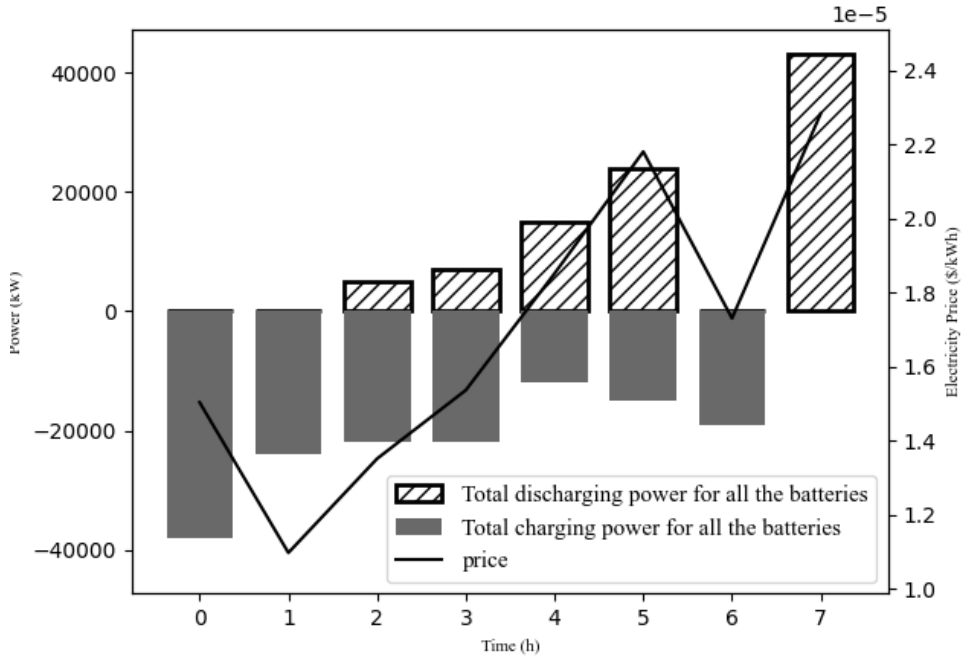


Figure A- 2: Total generation of all batteries for initial estimation of β coefficients

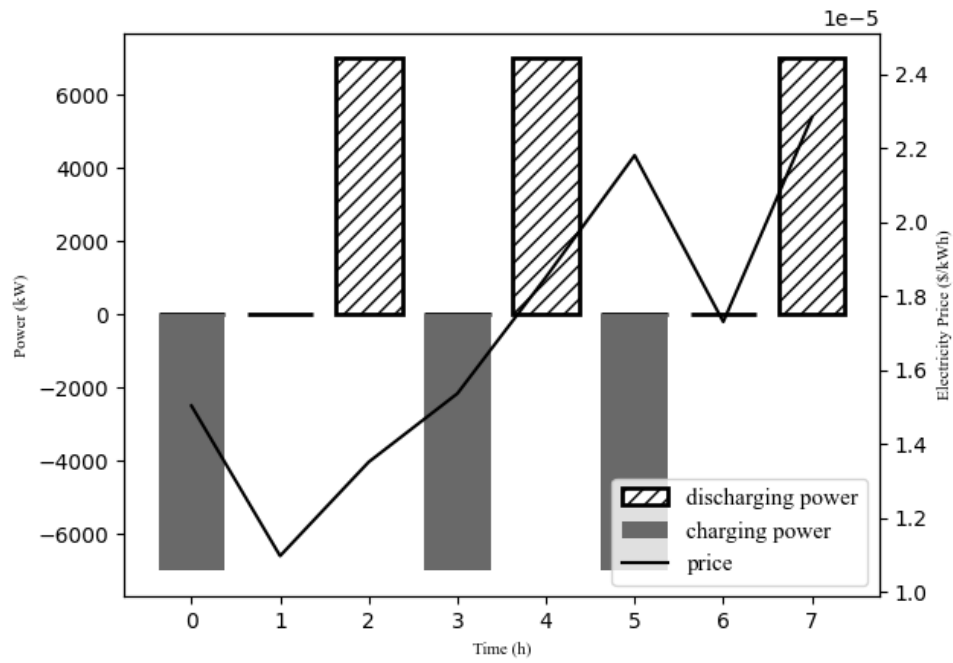


Figure A- 3: The generation of only one battery for 50% of β_0

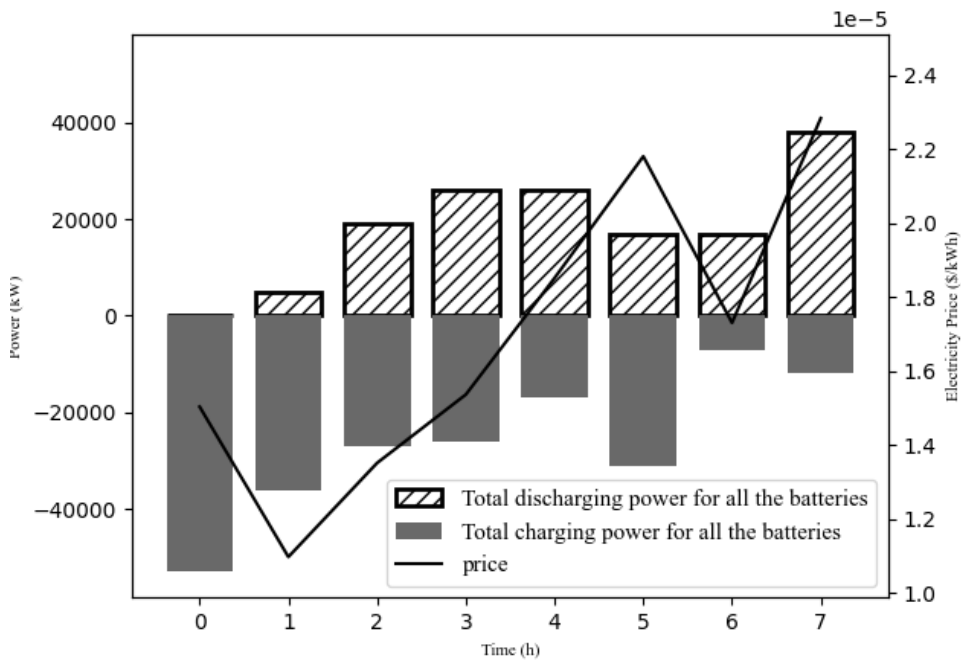


Figure A- 4: Total generation of all batteries for 50% of β_0

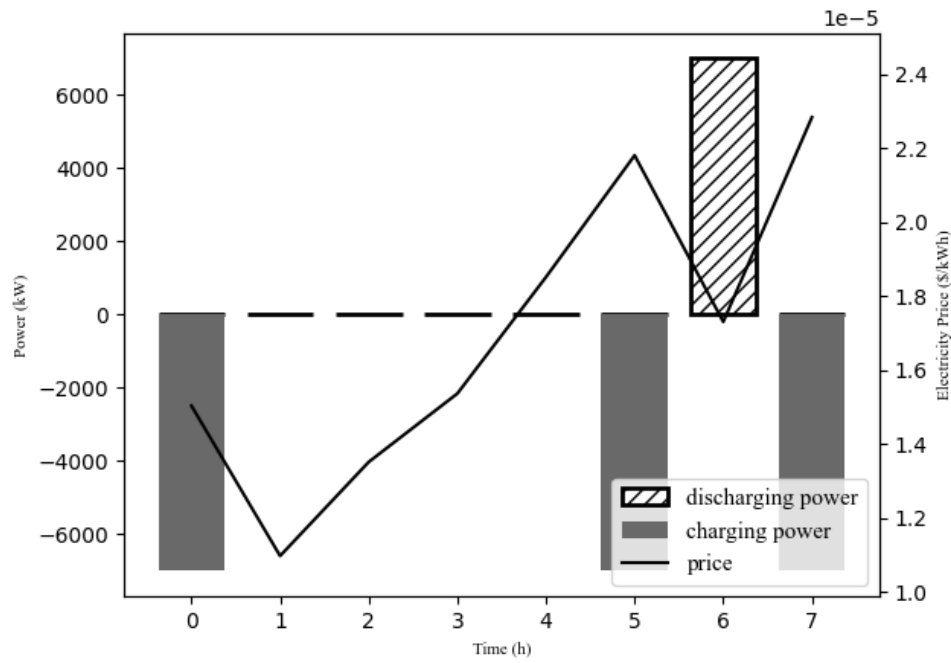


Figure A- 5: The generation of only one battery for 150% of β_0

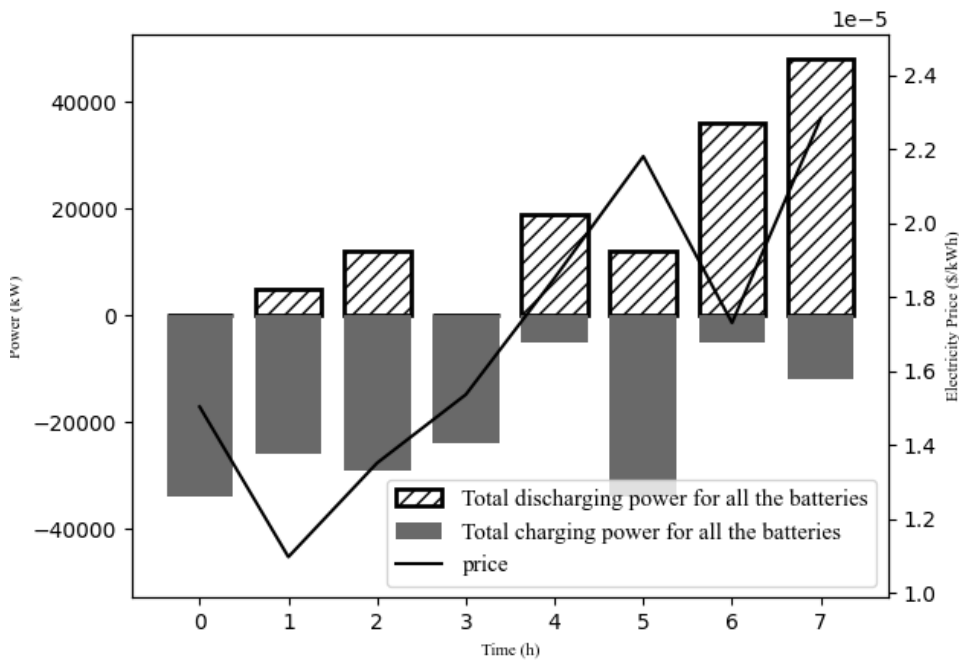


Figure A- 6: Total generation of all batteries for 150% of β_0

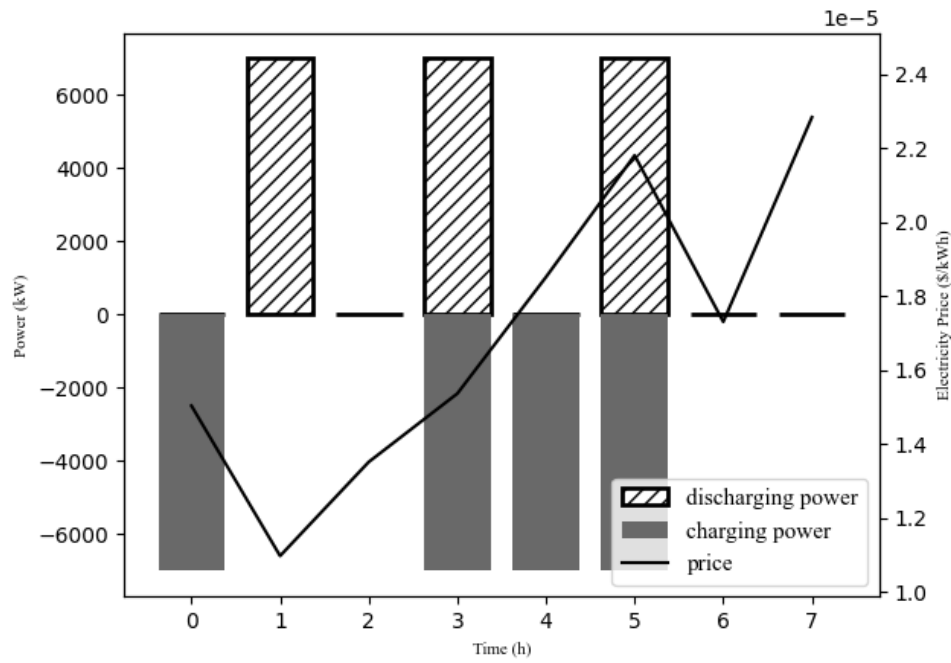


Figure A- 7: The generation of only one battery for 200% of β_0

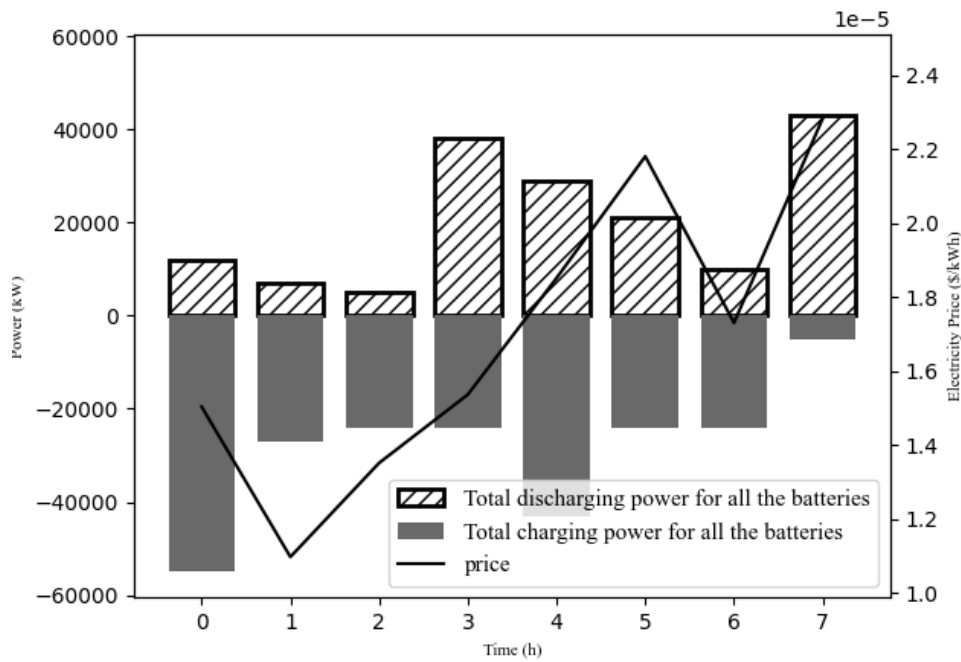


Figure A- 8: Total generation of all batteries for 200% of β_0

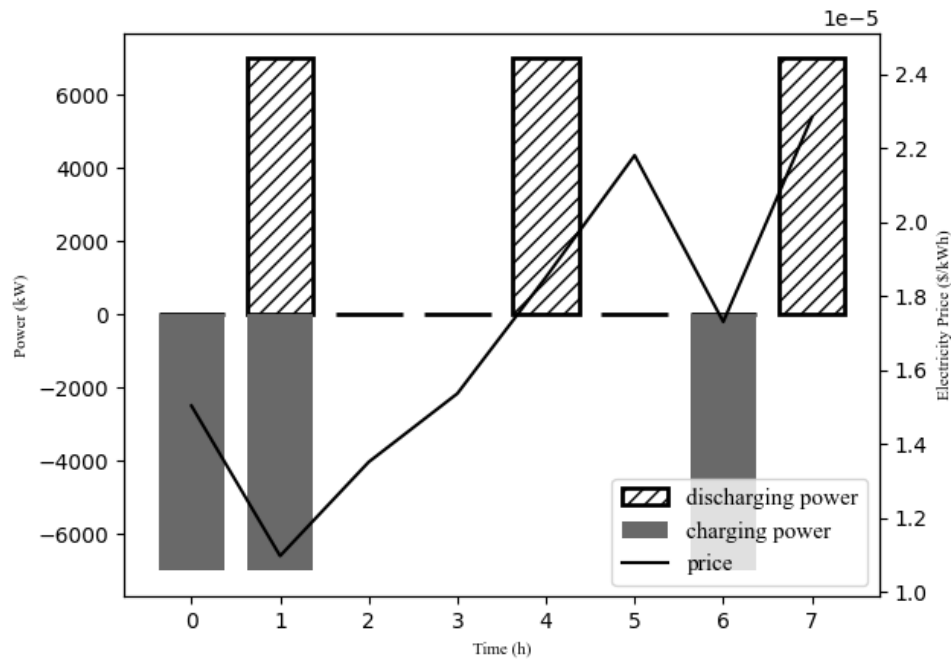


Figure A- 9: The generation of only one battery for 50% of β_1

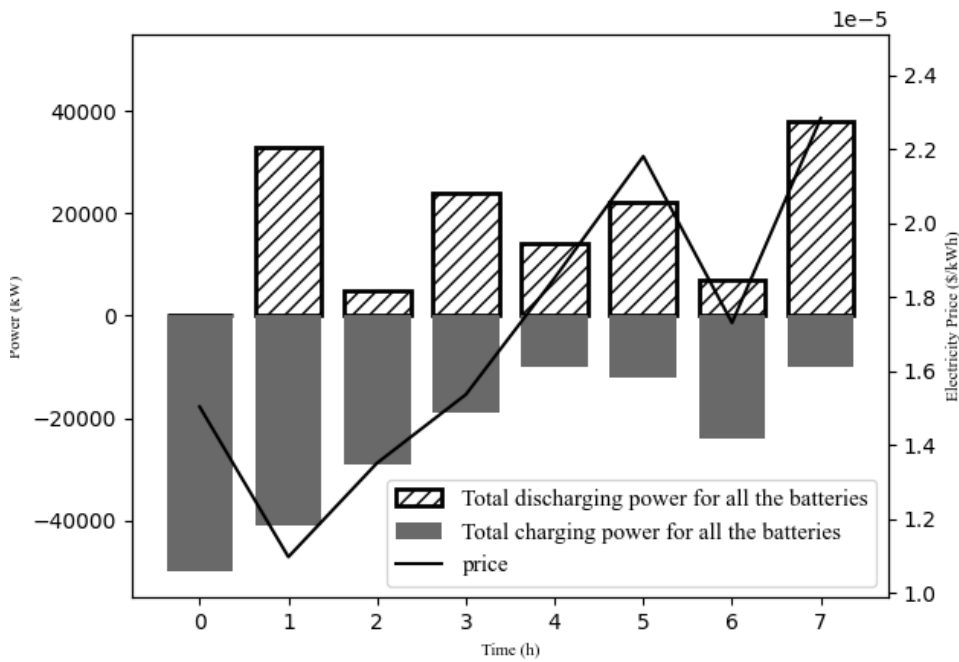


Figure A- 10: Total generation of all batteries for 50% of β_1

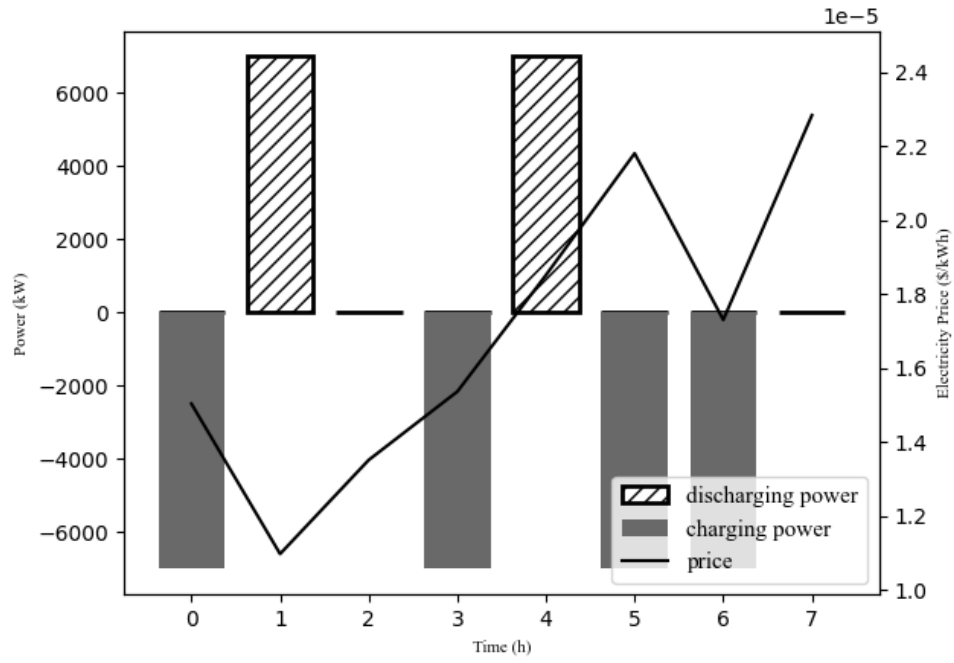


Figure A- 11: The generation of only one battery for 150% of β_1

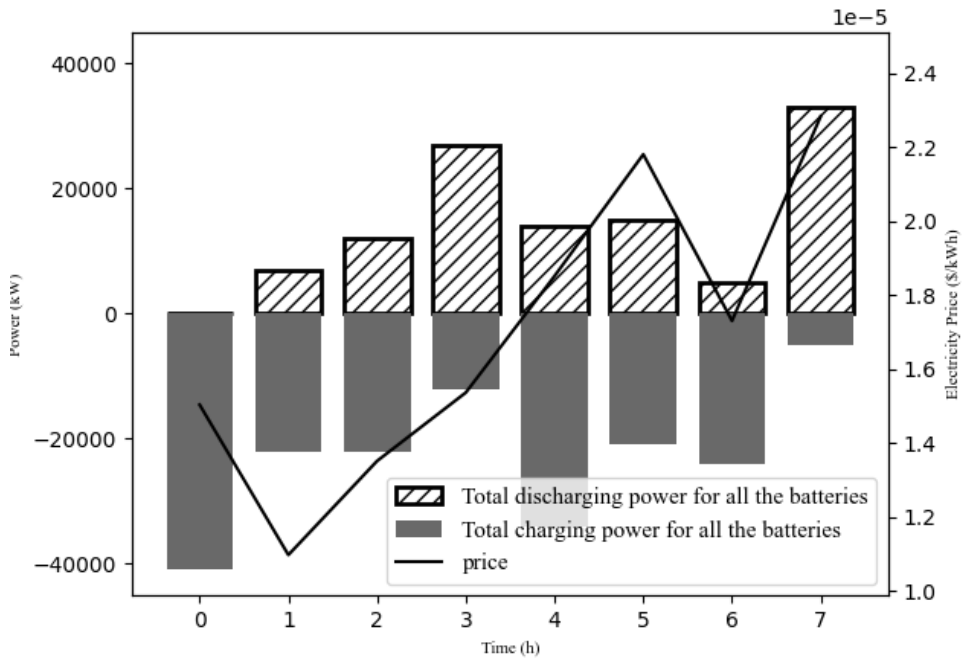


Figure A- 12: Total generation of all batteries for 150% of β_1

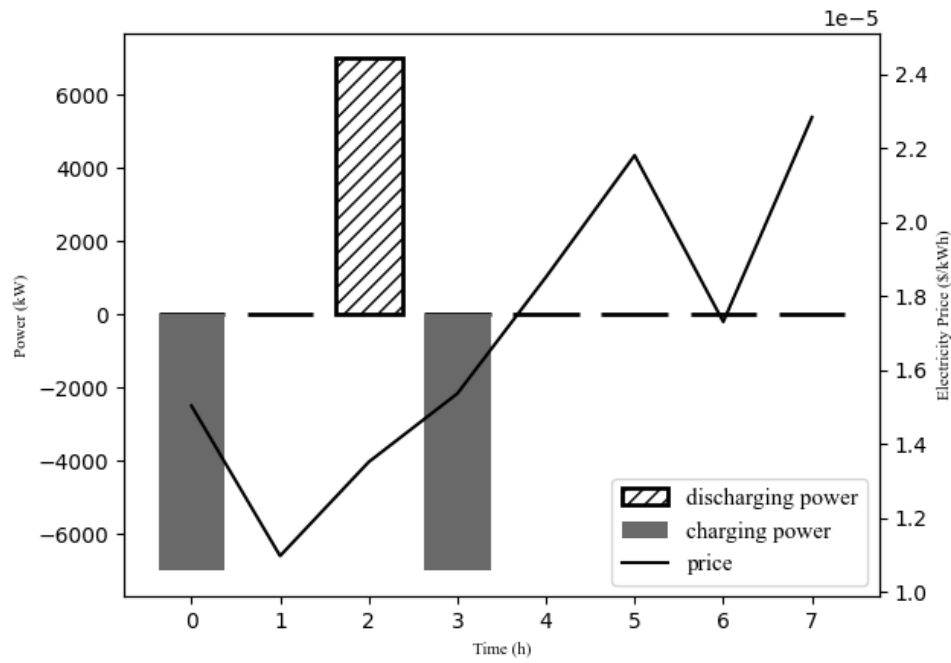


Figure A- 13: The generation of only one battery for 200% of β_1

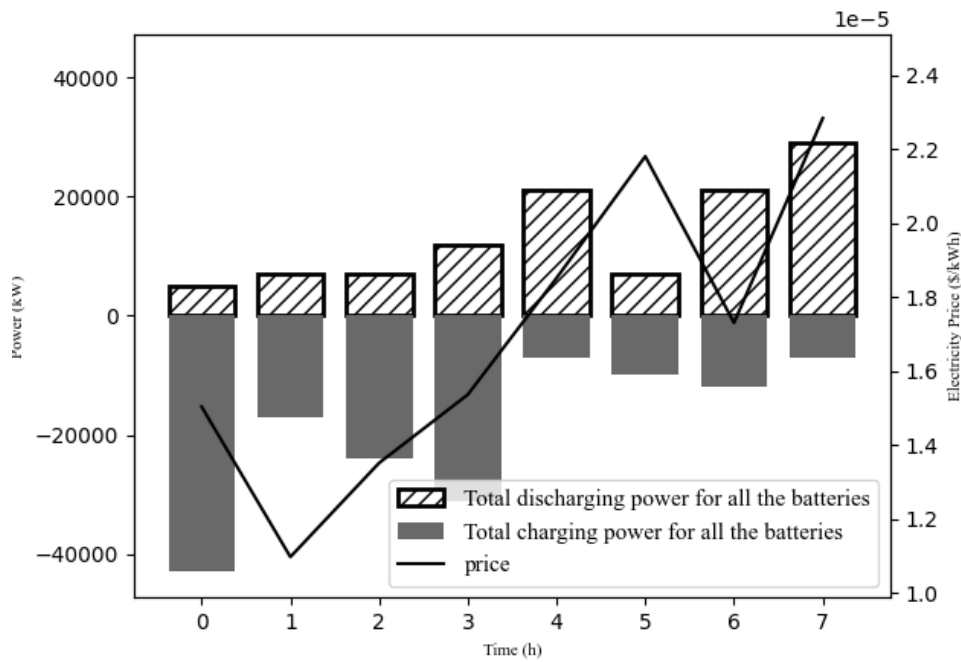


Figure A- 14: Total generation of all batteries for 200% of β_1

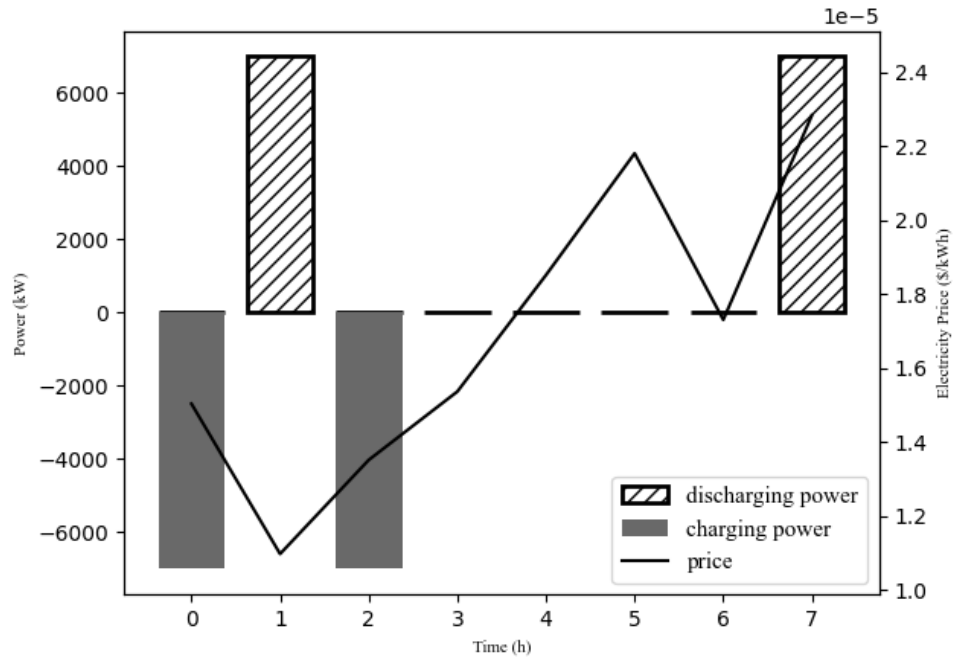


Figure A- 15: The generation of only one battery for 50% of β_2

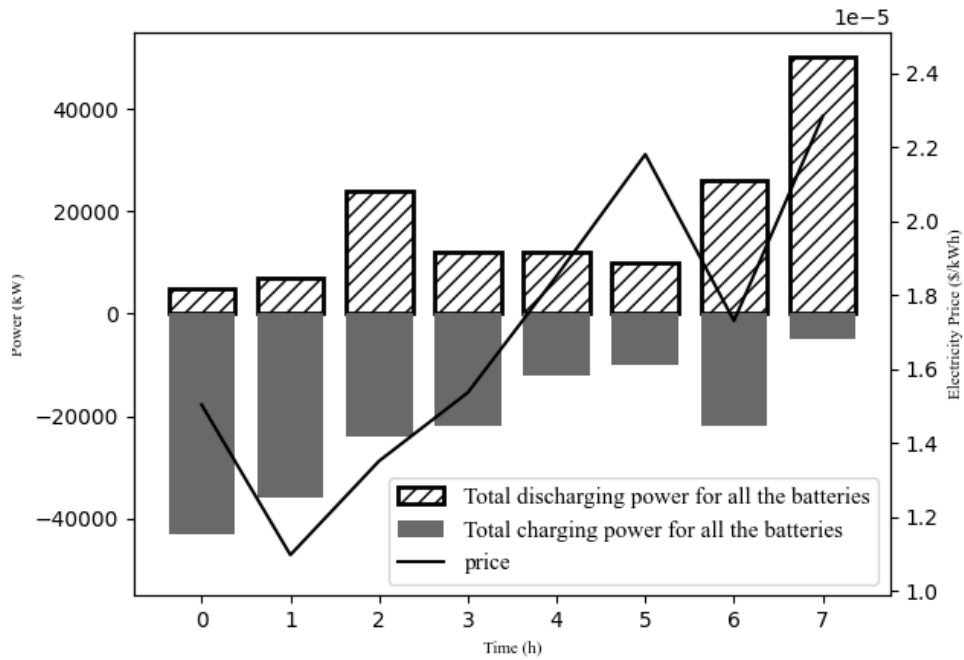


Figure A- 16: Total generation of all batteries for 50% of β_2

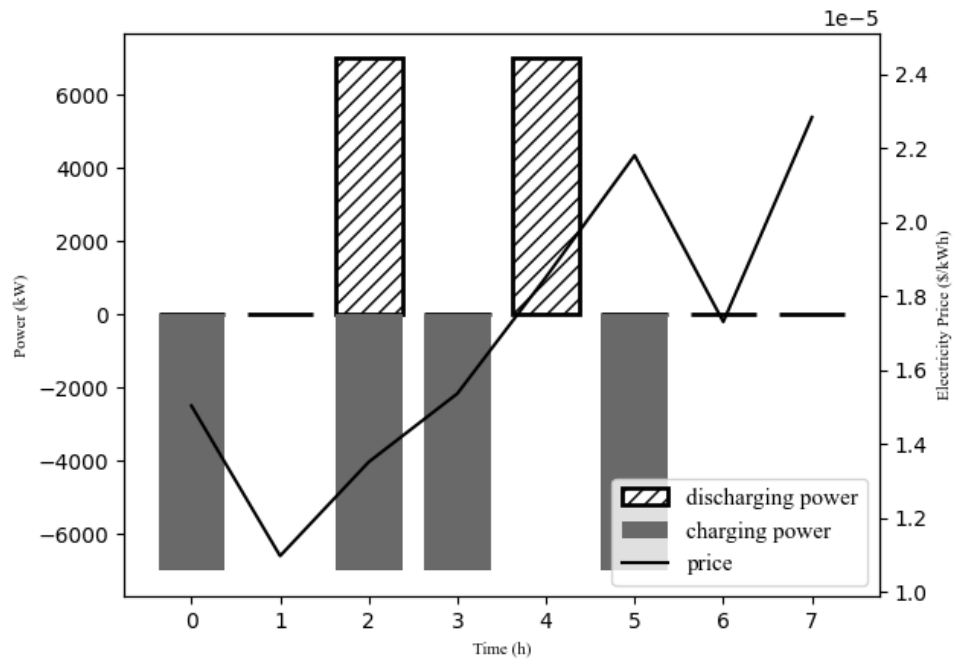


Figure A- 17: The generation of only one battery for 150% of β_2

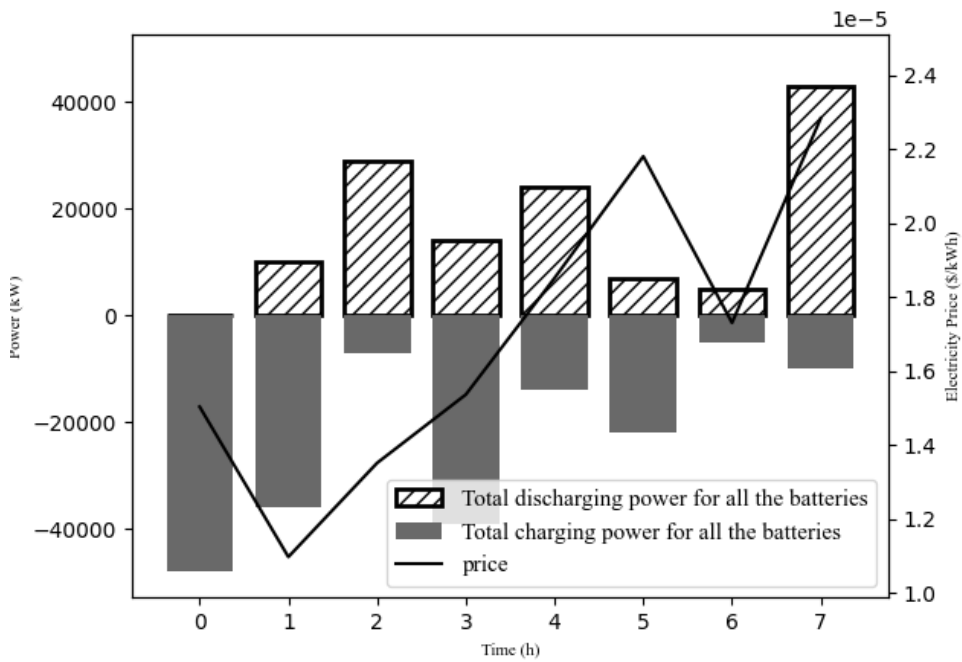


Figure A- 18: Total generation of all batteries for 150% of β_2

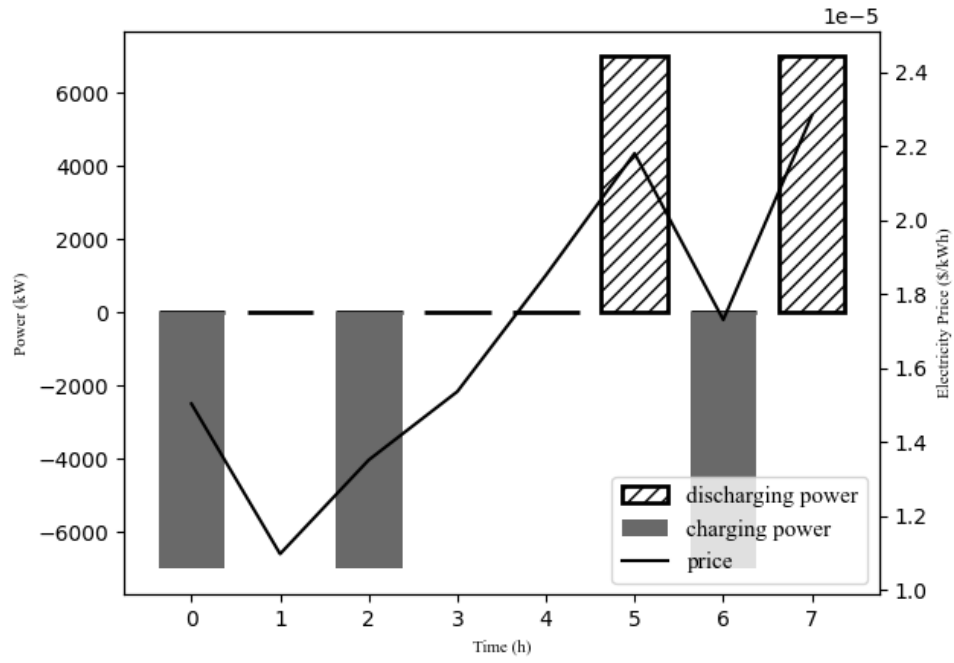


Figure A- 19: The generation of only one battery for 200% of β_2

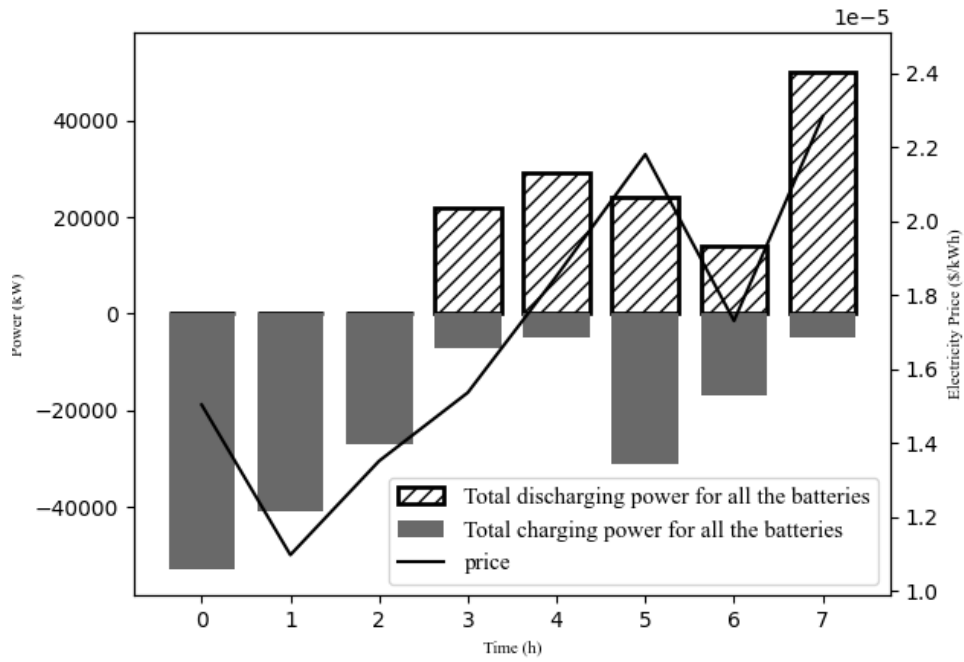


Figure A- 20: Total generation of all batteries for 200% of β_2

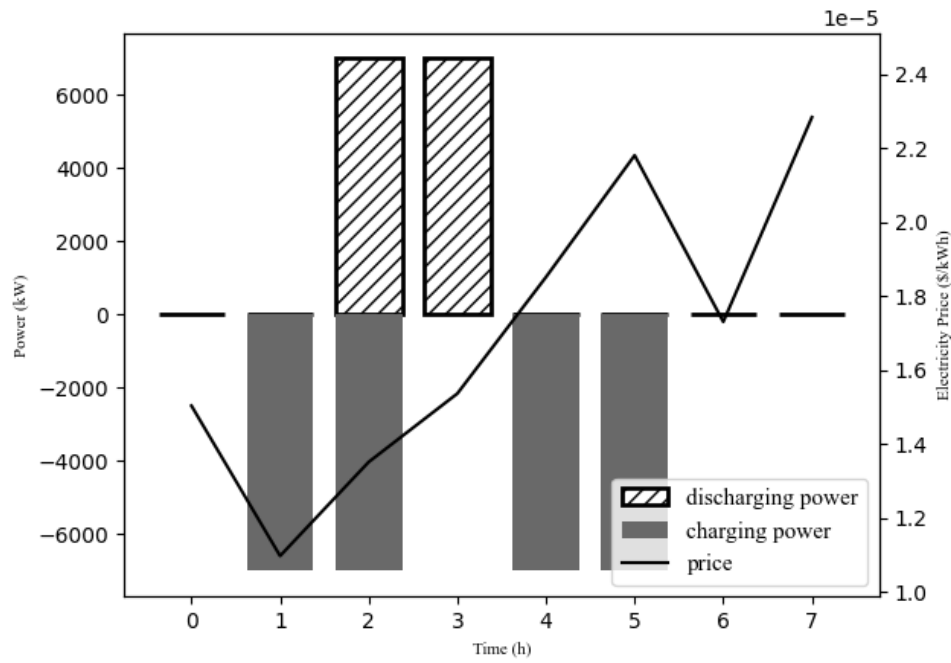


Figure A- 21: The generation of only one battery for 50% of β_3

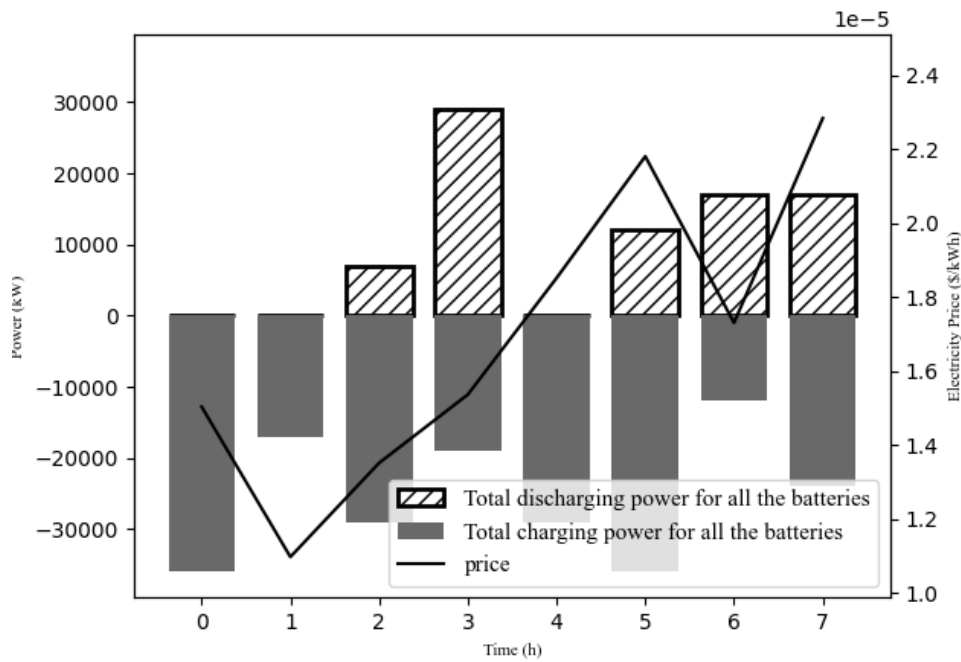


Figure A- 22: Total generation of all batteries for 50% of β_3

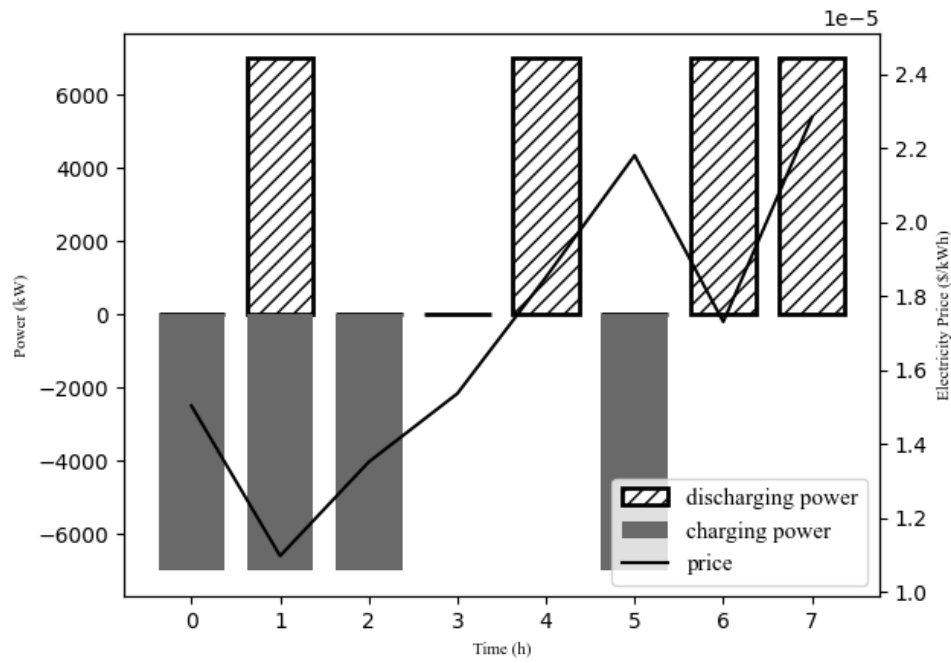


Figure A- 23: The generation of only one battery for 150% of β_3

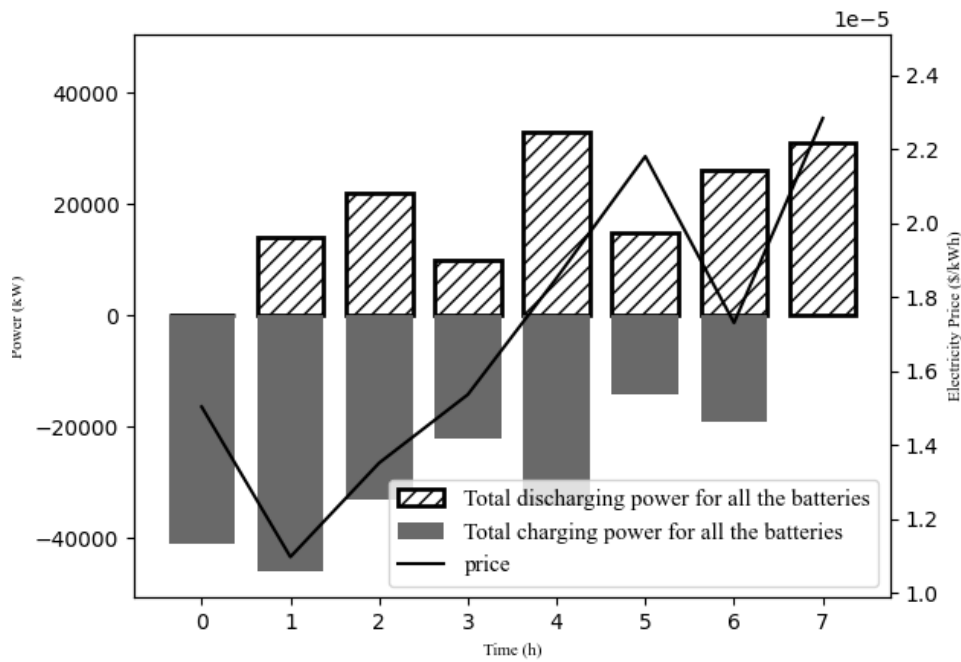


Figure A- 24: Total generation of all batteries for 150% of β_3

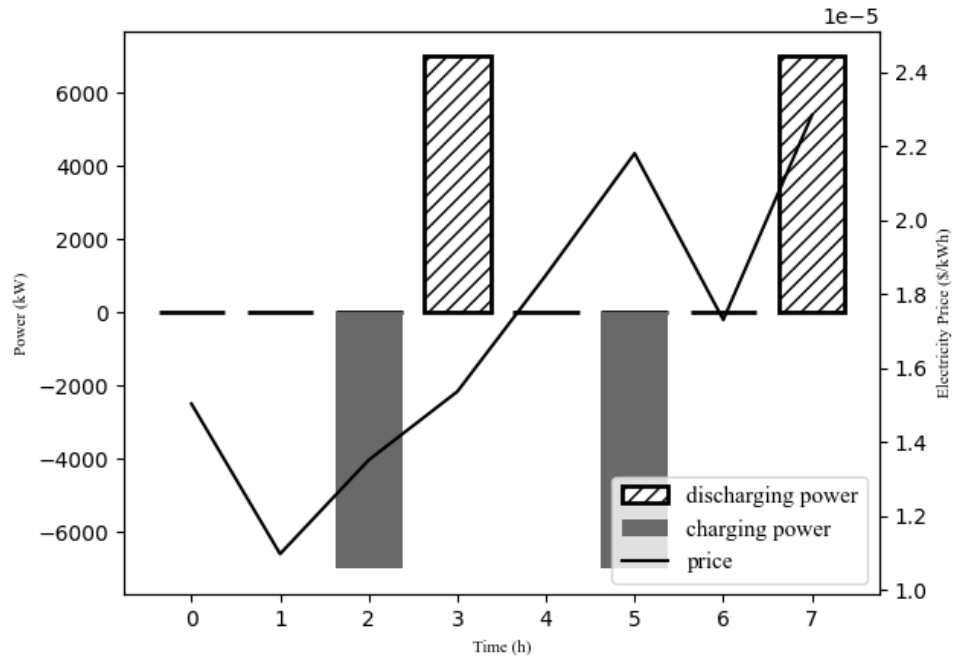


Figure A- 25: The generation of only one battery for 200% of β_3

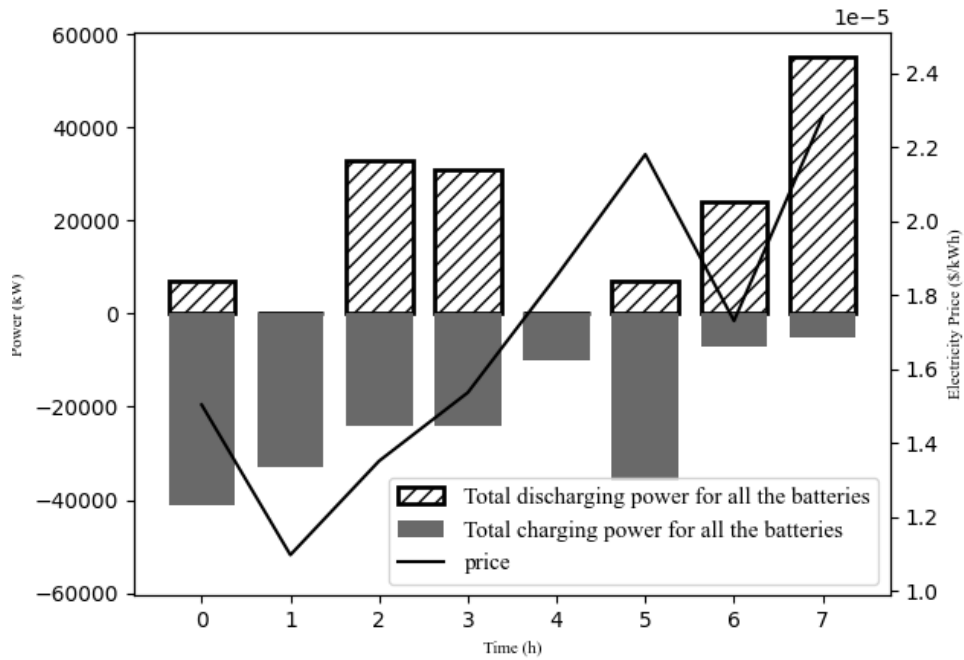


Figure A- 26: Total generation of all batteries for 200% of β_3

Appendix B: Sensitivity analysis, a systematic approach

beta1	beta2	beta3	Actual_obj_val	Actual_penalty1	Actual_penalty2	Actual_penalty3	Energy(D-Wave-reported)
0.01	0.01	0.01	39.17	0.81	707658.92	125.44	707824.34
0.01	0.01	1	32.63	0.53	544494.81	16384.00	560911.96
0.01	0.01	100	38.27	0.68	876183.78	6400.00	882622.73
0.01	1	0.01	39.37	0.67	62015191.00	0.81	62015231.85
0.01	1	1	35.79	0.67	71341902.00	33856.00	71375794.46
0.01	1	100	33.06	0.58	75998221.00	28900.00	76027154.64
0.01	100	0.01	37.08	0.64	5404709500.00	125.44	5404709663.16
0.01	100	1	33.48	0.65	7949313100.00	0.00	7949313134.13
0.01	100	100	32.18	0.54	6875934200.00	324900.00	6876259132.72
1	0.01	0.01	33.95	61.00	647858.11	3893.76	651846.82
1	0.01	1	33.79	66.00	609207.14	0.00	609306.93
1	0.01	100	36.05	63.00	828476.50	8100.00	836675.55
1	1	0.01	34.98	67.00	51291336.00	6658.56	51298096.54
1	1	1	38.05	85.00	60930628.00	380689.00	61311440.05
1	1	100	36.79	79.00	74847740.00	324900.00	75172755.79
1	100	0.01	36.25	58.00	5413247300.00	0.00	5413247394.25
1	100	1	37.25	65.00	6863933600.00	67782289.00	6931715991.25
1	100	100	33.63	54.00	6435918900.00	62500.00	6435981487.63
100	0.01	0.01	39.13	7000.00	626063.75	7464.96	640567.84
100	0.01	1	34.31	5800.00	634805.69	1.00	640641.00
100	0.01	100	34.23	6300.00	570598.48	6400.00	583332.71
100	1	0.01	37.84	7100.00	76912484.00	68486.89	76988108.73
100	1	1	36.62	7200.00	67554809.00	16384.00	67578429.62
100	1	100	33.52	5300.00	75098194.00	0.00	75103527.52
100	100	0.01	32.23	5700.00	6620471600.00	768778.24	6621246110.47
100	100	1	36.21	6700.00	6800738700.00	11025.00	6800756461.21
100	100	100	36.04	7000.00	5966577000.00	33177600.00	5999761636.04